Meroterpenes from *Dichrostachys cinerea* Inhibit Protein Farnesyl Transferase Activity

Christophe Long,[†] Laurence Marcourt,[†] Roselyne Raux,[‡] Bruno David,[†] Christelle Gau,[†] Christophe Menendez,[†] Min Gao,[†] Marie-France Laroche,[†] Philippe Schambel,[§] Clément Delaude,[⊥] Frédéric Ausseil,[‡] Catherine Lavaud,[∥] and Georges Massiot*[,†]

Joint Service Unit No. 2597 and Joint Service Unit No. 2646, National Center for Scientific Research (CNRS)-Pierre Fabre, Sciences and Technologies Institute of Medicine of Toulouse, 31432 Toulouse, France, Pierre Fabre Research Center (CRPF), Molecular Informatics Unit, 17 Avenue Jean Moulin, 81106 Castres, France, Centre de Recherche Phytochimique, Université de Liège, Institut de Chimie-B6, Sart Tilman, B-4000-Liège I, Belgium, Joint Research Unit No. 6229, National Center for Scientific Research, Reims Molecular Chemistry Institute, Laboratoire of Pharmacognosy, Reims Champagne-Ardenne University, 51097 Reims, France

Received March 7, 2009

Eighteen new meroterpene derivatives, dichrostachines A−R (**1**−**18**), have been isolated from the root and stem barks of *Dichrostachys cinerea*, and their structures determined by spectroscopic means and molecular modeling. From a biosynthetic standpoint these compounds arise from a Diels−Alder reaction between a labdane diene of the raimonol type and a flavonoid B-ring-derived quinone. The hypothesis was tested by the partial synthesis of similar compounds by simply mixing methyl communate and a synthetic flavonoid quinone. The hemisynthetic compounds were shown by NMR to have configurations different from those of the natural products, thus allowing a refinement of the biosynthesis hypothesis. Most of the compounds were assayed for their ability to inhibit the enzyme protein farnesyl transferase. The most active compounds exhibited IC_{50} and cytotoxicity values in the 1 μM range.

Protein farnesyl transferase (PFTase) plays an important role in the post-translational prenylation of several intracellular proteins. If the PFTase substrate is GTPase Ras, which is found in more than a third of human cancers in its mutated form, then the prenylation activity is inhibited, with functional consequences for the Ras-transformed cell phenotypes. As a result, PFTase inhibitors have been developed as potential anticancer drugs, by either rational design or random screening of chemical or natural product libraries.[1] Manumycin,[2] ajoene,[3] and methyl ganoderate A[4] are examples of natural products active on the PFTase enzyme. In the course of a large-scale screening of plant extracts aiming at finding new inhibitors of this enzyme, we came across a bioactive fraction from the root bark of *Dichrostachys cinerea* (L.) Wight & Arn. The plant is a spiny acacia-like treelet belonging to the Leguminosae family, common in Africa, from the sub-Saharan part to the south.[5] It grows in disturbed areas and impoverished soils and is sometimes planted as a defensive thorny fence. In some places, it forms invasive and impenetrable thickets and represents a nuisance. Numerous uses have been found for *D. cinerea* in traditional medicine.[6] The roots are used as a diuretic, febrifuge, antivenom, and antirheumatic and against leprosy. The trunk bark is believed to be a taeniafuge, antivenom, and antidysenteric and to be active against tooth decay and leprosy. The leaves are used to treat eczema, abscesses, measles, and rheumatism. Fresh twigs with leaves are recommended to prevent miscarriage. The fruit is utilized for the prevention of otitis, umbilical hernia, and malaria in children. Despite all these interesting properties, chemical investigations on the plant are scant and mostly limited to tannins, with the noticeable exception of a very recent preliminary report on the antitumor activity of some still unindenfied constituents.[7] In the present study, we isolated a novel flavono-labdane, which was named dichrostachine A, and given the originality of the compound and the lack of significant phytochemical investigations on the genus, it was decided to search for other secondary metabolites in various parts of the plant, resulting in the identification of 18 compounds belonging to the same group. They all had in common an association between a laddane and a flavonoid following an unprecedented Diels−Alder-type reaction that could be mimicked in an attempted partial synthesis of the skeleton of these new meroterpenes.

Results and Discussion

Fractionation of the EtOAc extract of the root bark was performed first by a liquid−liquid partition between hexanes and MeOH followed by MPLC of the MeOH soluble part, completed by semipreparative LC on C_{18}. All the successively obtained fractions were assayed against PFTase, and after the C_{18} fractionation, most of the activity could be attributed to a single compound, for which we propose the trivial name dichrostachine A (**1**). This compound showed a pseudomolecular ion peak at *m*/*z* 641.4 $[M + Na]^+$ in the positive ESI mode and a prominent fragment at *m*/*z* 337 corresponding to the loss of 304 mass units ($C_{20}H_{32}O_2$). High-resolution MS was obtained in the negative mode and confirmed the $C_{36}H_{41}O_9$ and $C_{16}H_9O_7$ composition for the quasimolecular ion $[M - H]^-$ and fragment, respectively. The UV spectrum showed two maxima, at 210 and 264 nm, with tailing down to 350 nm; in basic medium (MeOH, NaOH) the second band was displaced at 275 nm and absorptions appeared at 325 and 380 nm. The IR spectrum displayed strong OH vibrations at 3435 cm^{-1} and carbonyl bands at 1710, 1651, and 1609 cm^{-1}. The ^1H and ^{13}C NMR spectra (Table 1) were recorded in $CDCl_3$, acetonitrile-d_3, and methanol-d_4, and they showed signals for seven olefinic protons, one methoxy, one methyl on a trisubstituted double bond, and two "angular" methyl groups at unusually high field (δ 0.58 and 0.61). In $CDCl_3$, the ^{13}C NMR spectrum could be fully resolved into 36 signals, including four CH_3, eight CH_2, 10 CH, and 14 quaternary carbons, matching a $C_{36}H_{38}$ partial formula, thus leaving four exchangeable OH protons. In $CDCl_3$, some line broadening due to conformational mobility was observed, and since no improvement was obtained upon heating, "high-resolution" spectra had to be run in acetonitrile-d_3 and methanol-d_4, where the phenomenon was not observed with the same intensity. The analysis of these data was done using COSY, HSQC, and HMBC experiments, and despite severe overlap, this rapidly revealed the presence of a drimane subunit with a hydroxy group at C-7, an exomethylene at C-8,17, and a hydroxymethylene group at C-4. A substituted methylene group resided at C-9. The linkage of the methylene to an isoprene unit permitted us to propose a labdane skeleton; this latter isoprene unit was part of a six-membered ring. Interestingly, this ring contained

* To whom correspondence should be addressed. Tel: +33-532341402. 5-34321414. E-mail: georges.massiot@cnrs-dir.fr.
[†] Unité CNRS-Pierre Fabre 2597.
[‡] Unité CNRS-Pierre Fabre 2646.
[§] CRPF.
[⊥] Université de Liège.
[∥] Unité CNRS 6229.

10.1021/np900095z CCC: $40.75

Table 1. ^{13}C NMR Data of Compounds **1**−**8**

carbon	1	2	3	4	5	6	7	8
1	38.0	46.5	37.8	41.7	37.4	49.6	43.1	37.8
2	18.4	64.5	18.7	65.6	18.1	63.7	64.3	17.4
3	34.9	49.7	41.2	50.7	36.4	50.2	55.9	31.9
4	37.6	33.9	32.6	34.9	46.6	33.9	33.7	49.3
5	46.2	52.8	53.3	44.1	47.2	55.7	45.0	45.5
6	33.0	32.5	33.0	33.5	35.3	19.6	18.9	35.3
7	73.1	72.4	72.6	69.7	72.3	43.2	38.1	72.5
8	148.8	148.7	149.5	151.5	149.3	72.3	74.8	148.2
9	51.3	50.7	51.4	79.8	52.2	56.0	78.5	51
10	39.2	40.1	38.8	46.6	38.4	40.7	44.7	38.1
11	24.0	23.8	23.6	30.9	23.6	26.1	31.4	23.7
12	40.2	40.8	40.7	39.3	40.8	42.7	40.4	39.8
13	140.2	139.4	139.4	144.2	139.6	139.8	144.1	139.8
14	116.2	117.1	117.1	118.7	117.1	118.3	117.7	117.2
15	26.8	26.3	26.2	26.7	26.3	25.9	25.3	26.9
16	23.2	22.0	22.0	25.5	22.6	25.4	23.6	23.2
17	104.4	104.1	103.4	108.2	104.0	22.5	24.3	105.3
18	17.4	21.3	20.2	22.9	15.5	21.3	21.4	13.7
19	71.2	32.5	32.3	34.2	180.5	32.6	33.0	206.2
20	14.4	14.2	13.1	17.1	13.5	15.0	17.2	14.2
2′	166.8	167.1	167.2	167.2	166.8	167.1	167.0	166.6
3′	109.5	108.7	108.7	110.2	108.8	108.7	108.9	109.4
4′	181.5	181.2	181.2	182.7	181.2	181.3	181.6	181.4
5′	162.1[a]	162.0	162.0	162.5	162	161.7	161.7	162.1
6′	100.6	99.9	99.6	100.4	100.1	99.6	99.3	100.6
7′	163.7[a]	165.8	165.9	165.6	165.4	166.4	165.4	164.3
8′	95.1	94.6	94.2	94.7	93.8	94.2	93.7	94.9
9′	157.2	157.2	157.3	158.5	157.3	157.7	157.9	157.2
10′	105.1	104.3	104.0	104.9	104	103	103.7	104.9
1″	60.4	60.0	60.2	63.7	60.5	62.2	62.7	60.4
2″	192.6[a]	193[a]	193.0[a]	194[a]	192.9	192.9	192.8	192.5
3″	110.0	109.7	109.6	111.3	109.6	109.8	110.3	109.9
4″	159.6	160	160.0	161.6	160.0	160.3	160.7	159.6
5″	193.4[a]	193.2[a]	193.3[a]	194.5[a]	193.5	193.8	193.9	193.5
6″	42.5	42.2	42.4	44.1	42.5	42.5	43.1	42.5
OMe	56.6	56.1	55.9	57.1	56.1	55.9	55.9	56.6

[a] These resonances can be exchanged within the same column.

a trisubstituted double bond, which could be the locus of a theoretically acceptable retro Diels−Alder reaction (RDA), the result of which would be diterpene **A**, the molecular weight of which (304: $C_{20}H_{32}O_2$) exactly matched the observed MS fragmentation. This six-membered ring presented NMR signals used as "handles" for further construction: an olefinic proton at δ 5.24, coupling with two well-separated signals at δ 2.19 and 2.62, themselves coupling with a triplet at δ 3.81 (J = 9 Hz); on the other side of the double bond, a broad signal at δ 3.2 (δ_C 40.2) corresponded to H-12 (diterpene numbering) and linked this part of the molecule to the drimane core. The system was consolidated by the observation of an olefinic methyl at δ 1.9 (δ_C 23.2), which showed HMBC couplings with the two sp^2 carbons at δ 116.2 and 140.2 and with the methine at δ 40.2. Using these as reference signals, the analysis was pursued in a more elaborated model implying two ketone carbonyls at δ 192.6 and 193.4, a trisubstituted double bond (δ_C 110, 159.6), a methoxy at δ 56.6, and a quaternary sp^3 carbon atom at δ 60.4. The HMBC experiment and the chemical shifts of the sp^2 carbons showed that the double bond was part of a vinylogous methyl ester. All the HMBC correlations indicated annealation of partial formula B to a six-membered ring of the diterpene moiety, thus accounting for a $C_{27}H_{37}O_5$ formula for this part of the molecule with a single substitution point left at the angular position of the decalin-dione ring system. At that stage, there was a $C_9H_5O_4$ fragment unaccounted for, and for which the only detected signals in the ^1H NMR spectrum were three "singlets" at δ 6.17, 6.30, and 6.42. A particular feature of the latter two signals, which corresponded to carbons at δ 100.6 and 95.1, was that their integration was less than one proton and diminished with time in methanol-d_4. This behavior and the set of ^{13}C NMR shifts for the unassigned signals led to the proposal that the $C_9H_5O_4$ moiety constituted a 2-substituted chromone. Due to line broadening and exchange, the only HMBC correlations that were detected concerned H-3′ with $^{2/3}J$ with one of the ketone carbonyls, with the neighboring C-4′, and with the quaternary carbon at the ring junction of the decalin. All these elements allowed the proposal of flat structure **1** for dichrostachine A, which appeared to be made of a labdane and a flavonoid unit.

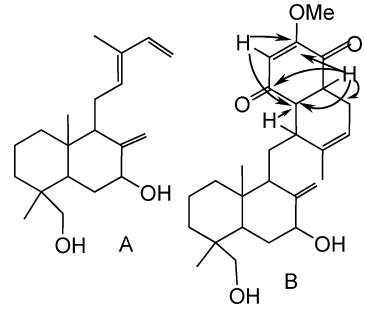

Dichrostachine A possessed eight stereogenic centers, six belonging to the labdane and two to the junction between the terpene and the flavonoid moieties. In the labdane part, observation of interproton coupling constants and ^{13}C NMR chemical shifts showed that the hydroxymethylene, OH-7, and the side chain were equatorial. Worthy of note were the ROEs observed between H-7, H-5, and H-9, which could be justified only in a *trans*-decalin with equatorial substituents at positions C-7 and C-9. The upper part of the molecule displayed three remarkable Overhauser effects: between H-3′ of the chromone residue and H-6″ situated at the ring junction on one hand and H-12 of the labdane part on the other, and between H-6″ and one of the diastereotopic C-11 protons. These observations allowed determination of the ring junction as *cis*, and despite the fact that *cis*-decalins may exist under two interconverting configurations, the three NOEs are compatible only with an all-*cis* arrangement of the chromone, H-6″, and C-11. The relative configuration of the two parts and the absolute configuration

Table 2. ^{13}C NMR Data of Compounds **9**−**18**

carbon	9	10	11	12	13	14	15	16	17	18	23	24
1	39	47.4	32.7	38.4	38.5	41.7	38.8	37.4	39.9	38.3	38.4	38.7
2	18.5	65	19.5	18.7	18.6	64.9	18.9	18.8	19.5	18.8	19.8	20
3	35.6	49.7	42.1	41.4	41.4	50.2	40.1	41	41.6	41.5	38.2	38.5
4	38.5	34.6	34	33.3	33.3	34.7	34	33.2	33.4	32.7	44.3	44.3
5	45.8	51.6	44.1	52.2	52.3	43.2	53.1	53	53	52.6	56.8	56.8
6	38.5	37.8	39.3	nd[c]	38.1	nd	32.6	32.6	34.3	32.9	26.3	26.2
7	204.4	202.4	207.6	203.8	202.4	206.8	72.8	72.7	73.4	72.9	38.8	38.7
8	148.7	147	152.7	nd	147.8	nd	149.4	149.6	149.7	150	147.2	147.9
9	55.2	52.6	79.9	53	53.5	79.2	50.8	51.2	54.1	55	54.7	55.0
10	39.3	40.1	44.9	38.6	38.4	45.8	37.4	38.9	41.8	38.6	41.2	41.0
11	27.1	25.9	31.8	25.3	25.6	nd	23.5	24.2	73	22.8	26.0	25.0
12	43.9	41.4	39.6	40.6	41.6	38.9	43.4	47.5	39	125.3	43.2	45.5
13	140.8	139.3	143.7	139.4	139.8	nd	138.9	136.5	130	132.5	135.8	138.5
14	118.6	118.1	119.2	117.8	117.7	118.9	119.4	122.7	124.9	36	120.0	118.4
15	27.2	26.7	27.2	26.8	26.7	nd	23.8	23.5	22.3	25	20.6	25.2
16	24.8	24.1	25.1	24.1	24.2	25	22.2	22.3	23.8	14.5	24.2	23.8
17	120.4	120	120.8	118.8	118.8	120.9	103.6	103.2	105.7	104.9	107.5	106.9
18	16.7	21.4	21.5	20.4	20.4	22.5	20.6	20.3	20.9	20.7	28.8	28.8
19	70.8	32.5	33.3	32.3	32.3	33.3	32.6	32.3	33.2	32.5	177.7	177.6
20	14.4	14.5	16.5	13.6	13.6	17.5	13.5	13.2	14.5	13.3	12.1	12.1
2′	167	166.2	168	166	166.3	167.5	168.2	175	168.4	160	163.2	162.2
3′	109.7	109.9[a]	110.4	109.6	109.7	110.2	108.8	109.6	107.5	112	113.5	110.3
4′	181.9	181.2	182.9	181.5	181.2	nd	181.7	181.6	182	180.5	176.8	178.2
5′	162.4	162.3	nd	nd	161.7	nd	162	162	161.7	162.2	160.9	160.4
6′	100.8	100.7	100.6	100.3	99.3	99.3	99.6	99.3	98.9	97.8	96.2	96.5
7′	166.4	163.9	nd	nd	166.1	161.3	165	165.2	164.6	165	164.0	164.2
8′	95.2	95	95	94.7	92.5	93	94.8	94.4	93.6	93.3	92.5	93.0
9′	158.2	156.9	nd	nd	157	nd	157.3	157.4	158.1	157.8	159.7	160.3
10′	104.7	105	105	104.7	105.3	nd	104.5	104.2	104.1	103.3	108.8	108.6
1″	62.1	60.8	63.7	60.9	61	nd	57.6	49	57.5	119	61.0	61.1
2″	193.3	192.1[b]	193.9[a]	192.1[a]	192[a]	194	194.5	151.8	197.5	148	196.3	195.4
3″	110.5	109.7[a]	111.4	109.6	109.7	111.1	100.4	127.2	103	115.6	112.3	112.3
4″	160.7	159.7	161.7	159.6	159.6	166.8	176.2	198.8	171.1	112.3	163.8	165.7
5″	194.2	193.3[b]	194.8[a,b]	193.4[a]	193.1[a,b]	194	68	73.9	95	143	192.9	139.5
6″	43.3	42.5	44.1	42.8	42.6	43.9	33.6	34.9	39.1	125	46.7	119
OMe	57.1	56.7	57.3	56.6	56.5	56.3	56		56.3		51.2	51.2
OMe					56	57					56.5	55.9
OMe											56.6	56
OMe												56.9

[a,b] These resonances can be exchanged within the same column. [c] nd: not determined.

of the whole molecule will be dealt with after examination of all other molecules isolated from the plant and molecular modeling.

Compound **1** was accompanied by a host of structurally closely related molecules, which were isolated and purified in order to correlate structure with activity in this new series. Two batches of the plant with slightly different compositions, despite a common origin, were used, and the isolation of the new compounds is detailed in the Experimental Section. Thus, compounds **1**−**14**, raimonol, and **19** were found in the root bark, **2**, **3**, **15**−**18**, and raimonol were found in the stem bark, and rhamnitrin[8] and myricitrin 3-*O*-α-L-rhamnoside[9] were the only compounds that could be characterized in the leaves. The occurrence of (+)-raimonol, a diterpene chemically correlated to *cis*-abienol of known absolute configuration and isolated from the exudates of *Nicotiana raimondii*,[10] brought further credence to the structural hypothesis and allowed a precise determination of the absolute configurations of **1** and related compounds on the basis of a common biosynthesis origin.

All the isolated compounds, except **18** and **19**, showed a quasimolecular ion in the same range, and their ^{1}H and ^{13}C NMR spectra displayed signals for a chromone as in dichrostachine A (**1**). As a working hypothesis, they could be considered as belonging to the same series. More precisely, compounds **1**−**5** and **8** contained raimonol skeletons at different oxidation levels. Compounds **6** and **7** had the exomethylene double bond hydrated, and compounds **9**−**14** had a C-7 keto functionality. All the NMR assignments allowing such conclusions were based on the analysis of homonuclear and internuclear 2D NMR experiments; their results are collated in Tables 1 and 2.

Dichrostachine B (**2**), an isomer of **1**, was obtained by repeated C_{18} fractionation of a fraction of lower polarity than the one from which **1** was isolated. This compound displayed spectra similar to those of **1**, including MS with the same quasimolecular ion at *m*/*z* 617 $[M - H]^-$ and identical fragmentation pattern (*m*/*z* 313) in the negative mode. Structure **2** was proposed mainly upon methyl group counting and also owing to observation of a deshielded H-2 in the labdane part. The high-field section of the ^{1}H NMR spectrum showed signals for three tertiary methyl groups at δ 0.62, 0.68, and 0.74, with the latter two signals displaying three identical HMBC correlations with C-3, C-4, and C-5, pointing to a quaternary C-4 substituted with two methyl groups. The substitution at C-2 was ascertained by the deshielding of C-1 (δ 46.5 vs 38) and C-3 (δ 49.7 vs 34.9), both identified through their ^3J HMBC correlations with the tertiary methyl groups. The two alcohol functions were equatorial since H-2 showed NOEs with axial CH_3-18 and -20 on one side and H-7 with the angular H-5 on the other. As in compound **1**, NOEs were observed between H-3′ of the chromone and H-12 and H-6″; H-5, identified through the HMBC and HSQC experiments, was at an unusually high field, and this will be commented upon in the general discussion on stereochemistry ($\delta_{H\text{-}5}$ 0.18).

The molecular weight of compound **3**, dichrostachine C, was 16 amu lower than those of **1** and **2** (602 vs 618), suggesting that one of the alcohol functions was absent. The retro Diels−Alder fragmentation gave an ion at *m*/*z* 313 in the negative mode, showing that the "flavonoid" part of the molecule was intact and that the missing OH was in the terpene part. Besides minor chemical shift differences, the spectra of **2** and **3** were almost superimposable with the noticeable exception of the lack of deshielded signals for H-2 and C-2, allowing assignment of the structure of 2-deoxydichrostachine B for **3**. The same Overhauser effects were observed in the two compounds, as well as the same characteristic shielding for H-5, as a consequence of a similar relative arrangement of all stereogenic centers.

Compound **4**, like compounds **2** and **3**, was characterized by three high-field tertiary methyl groups in the ^{1}H NMR spectrum, suggesting that C-4 was substituted by two methyl groups. Its molecular weight was measured at *m/z* 634, i.e., 16 amu higher than observed for **2**, and corresponded to a $C_{36}H_{42}O_{10}$ formula (*m/z* 633 in the negative mode). According to the NMR spectra and despite some minor chemical shift differences, it was clear that all the elements of the upper part of the molecule, chromone and dihydronaphtalenedione, as well as the two alcohol functions at C-2 and C-7 and the exomethylene group were present in this molecule. Although the mass spectrum was richer in fragments than those of the previous molecules, the integrity of the "upper part" was again demonstrated by the MS fragmentation with a prominent ion at *m/z* 313. The location of the additional hydroxy group was settled by the observation of a correlation between CH_3-20 and a quaternary carbon atom at δ 79.8, either C-5 or C-9. The C-5 center was eliminated since the HMBC and HSQC experiments allowed its detection at δ 44.1, a much higher field than in the other compounds of the series, and this shielding could be explained by a steric γ-effect, meaning that the OH at positions C-9 and H-5 were both axial in a chair conformation. Compound **4** was thus 9-hydroxydichrostachine B, for which the name of dichrostachine D is proposed.

Compound **5**, named dichrostachine E, was isolated from the most polar fractions of the extract, and its molecular weight, 632, corresponded to a $C_{36}H_{40}O_{10}$ formula suggesting an additional oxygen atom and unsaturation. As the ^{1}H NMR spectrum of **5** showed signals for only two high-field methyl singlets, **5** could be the carboxylic acid corresponding to the primary alcohol function in **1**, and this was confirmed by observation of a three-bond CH correlation between one of the tertiary methyl groups and an acid carbonyl at δ 179, all other correlations in the HMBC experiments being in agreement with the gross structure of the series. The relative configuration at C-4 could be determined by the observation of a strong shielding for the remaining methyl group (δ 15.5), indicative of an axial position and therefore equatorial for the carboxylic acid group. An NOE was detected between the two axially oriented methyls (CH_3-18 and CH_3-20).

Compounds **6** and **7**, dichrostachines F and G, were obtained from a fraction with polarity between those of **2** and **3**. Their molecular ions were respectively found at *m/z* 620 and 636, and the RDA peak was at *m/z* 313. In both compounds, an OH group was placed at C-2, as in **2**, to account for the deshielding of C-1. The most conspicuous feature of their ^{1}H NMR spectra and those of the other compounds was the absence of signals for the exomethylene group and the presence of an additional methyl singlet, observed at δ 1.01 in **6** and 1.21 in **7**. In compound **6**, this methyl group showed HMBC correlations with carbon signals at δ 43.2 (CH_2), 56.0 (CH), and 72.3 (C), indicating that it was on an oxygen-substituted quaternary carbon atom, flanked by a CH and a CH_2 group. Biogenetic considerations and analysis of all the COSY, HSQC, and HMBC correlations led to the proposal that the exomethylene bond was hydrated in **6** and **7**. In the two compounds, a strong shielding was observed for C-6 as a consequence of γ-shifts due to the OH and the methyl group at C-8. Compound **7** differed from **6** by an oxygen atom, placed at C-9, the ^{13}C NMR signal of which was identified by a three-bond correlation with CH_3-17, CH_3-20, and H-12; this substitution induced significant downfield shifts for C-11 ($\Delta\delta$ +7) and C-10 ($\Delta\delta$ +5) when compared with dichrostachine D. This tertiary alcohol function was deduced to be axial to account for the 8 ppm shielding of C-5, as a consequence of a 1,3-diaxial interaction, also a γ-effect. As in compounds **1**−**3**, ROESY interactions were observed between H-3′ and H-12 and -6″, settling the point of the relative configurations in the "upper" part of the molecule. As far as rings A and B of the diterpene were concerned, a series of ROEs between CH_3-17, CH_2-11, CH_3-20, and CH_3-18 left the axial orientation of the above-mentioned tertiary methyl and the equatorial nature of the side chain to be established. The same experiment revealed key ROEs between H-2 and the two axial methyls at C-4 and C-10, thus providing supplementary evidence for the OH orientation.

Compound **8**, dichrostachine H, was the only aldehyde in the series (δ 8.81). The molecular weight of 616 ($C_{36}H_{40}O_9$) indicated an additional unsaturation degree when compared to compounds **1** and **2**. The aldehyde function was placed at C-19, through observation of a correlation with tertiary CH_3-18, identified as axial because of its strong shielding (δ 13.7). Most chemical shifts in **8** were similar to those observed for the corresponding atoms in **1**, except for C-4 ($\Delta\delta$ +12), C-18 ($\Delta\delta$ −4), and C-3 ($\Delta\delta$ −3). As a direct consequence of oxidation and given the similarity of all other chemical shifts, the rest of the structure and the configuration were deduced to be as in dichrostachine A.

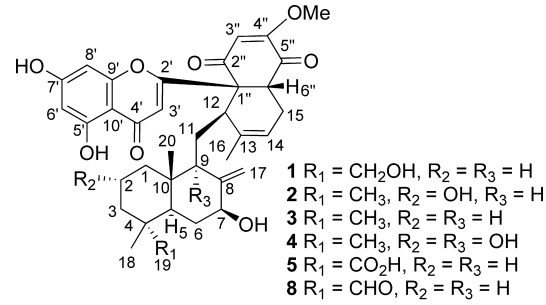

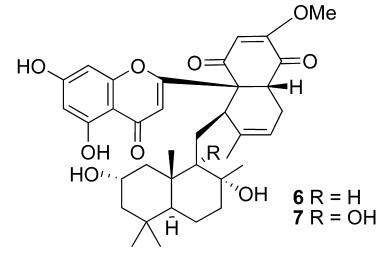

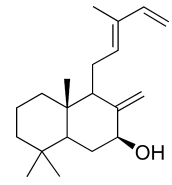

(+)-raimonol

Dichrostachines I−L (**9**−**12**) displayed spectroscopic properties analogous to those of the parent compounds but were distinguished from the latter by the presence of an additional double bond, as shown by MS. Dichrostachines I, J, and K were isomeric and displayed molecular ions at *m/z* 616 ($C_{36}H_{40}O_9$), while compound **12** had a $C_{36}H_{40}O_8$ composition (*m/z* 600). All these compounds showed the fragment at *m/z* 313 in the negative mode; in the positive mode, two fragments were generally observable at *m/z* 325, corresponding to the labdane plus a sodium atom, and *m/z* 337, corresponding to the flavonoid also with a sodium atom. The most striking difference between the NMR spectra of **9** and of its closest counterpart, dichrostachine A (**1**), was the downfield shifts of the H-17 exomethylene protons: δ 5.25/4.85 in **1** vs 5.84/5.25 in **9**. The oxymethine C-7 group was replaced by a ketone carbonyl at δ 204.4 ppm, thus explaining the shifts of CH_2-17 and of CH_2-6 appearing as part of an AMX system with a fairly large geminal coupling constant (J = 17.5 Hz). The only ^{13}C NMR signal for an oxygen-bearing sp^2 carbon atom was found at δ 70.8 and corresponded to C-19 (HMBC correlations with CH_3-18, C-3, and C-5), the rest of the NMR signals being very close to those of **1**, thus establishing the structure of **9** as 7-dehydrodichrostachine A. Despite repeated attempts and due to the limited amount of material, it was not possible to cleanly oxidize **1** into **9**. In a similar fashion, compound **10** was found to be analogous to dichrostachine B (**2**),

and the similarities between the ^{13}C NMR chemical shifts of C-2 in **2** and **10** (δ 64.5 and 65) indicated a similar configuration for these carbon atoms. The third isomeric compound, **11**, did not have an equivalent in the "reduced" series but showed similarities with compound **4**, both bearing a tertiary OH group at C-9, with compound **11** lacking the C-2 hydroxy group. Evidence for the structure was the deshielding of CH_2-17 due to the C-7 carbonyl group (δ 207.6), strong shielding of C-2 (δ 19.5), and substitution of C-9 with an OH, as shown by an HMBC correlation between C-20 and a tertiary carbon atom at δ 79.9 (C-9). The elemental composition of dichrostachine L (**12**) suggested that the only oxidized carbon on the labdane was C-7.

This set of compounds was accompanied with two related compounds, dichrostachines M and N (**13** and **14**), which were the only compounds in the series with one of the phenolic hydroxy groups being methylated. Compound **13** showed a molecular ion at *m*/*z* 614 and was thus identified as 7′-*O*-methyldichrostachine L (**12**). A special feature of its ^1H NMR spectrum recorded in $CDCl_3$ was the presence of a sharp resonance at δ 12.26 for a phenolic hydroxy proton, deshielded as a consequence of hydrogen bonding with the C-4′ carbonyl, therefore establishing the site of etherification. When the spectra were recorded in a mixture of $CDCl_3$ and methanol-d_4 to improve solubility, compound **13** showed noticeable instability and decomposed within 24 h into a mixture of at least five unidentified compounds. This behavior was not observed for the other compounds and seemed related to the etherification of one of the phenolic functions. The last compound in the series, **14**, derived from **4** since it showed C-7 as a ketone, C-2 and C-9 as oxymethines, and the methyl substitution on the phenol of the chromone ring. This compound was isolated in minute quantities and could not be further characterized.

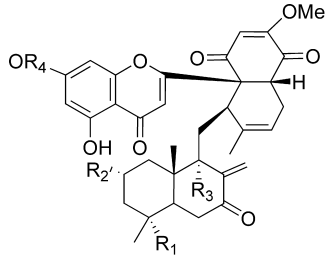

9 $R_1 = CH_2OH$ $R_2 = R_3 = R_4 = H$
10 $R_1 = CH_3$ $R_2 = OH$ $R_3 = R_4 = H$
11 $R_1 = CH_3$ $R_2 = R_4 = H$ $R_3 = OH$
12 $R_1 = CH_3$ $R_2 = R_3 = R_4 = H$
13 $R_1 = CH_3$ $R_2 = R_3 = H$ $R_4 = CH_3$
14 $R_1 = CH_3$ $R_2 = R_3 = OH$ $R_4 = CH_3$

A rapid investigation into the compounds of similar polarity present in the stem bark led to the isolation of dichrostachines B and C (**2** and **3**) as the major components, meaning that apparently these organs had low oxidation power as compared to the root. However, two other compounds directly linked to the above were isolated, presenting quite different structural features. Compound **15**, for which the name dichrostachine O is proposed, displayed a quasimolecular ion at *m*/*z* 603 in the negative mode, thus corresponding to a $C_{36}H_{43}O_8$ composition. As in all dichrostachines, an RDA fragmentation was observed and yielded an ion at *m*/*z* 315, suggesting reduction in the flavonoid part. NMR analysis showed little difference with the other compounds up to H-6″, which now appeared as a double triplet at δ 3.53, as a result of coupling with CH_2-15 and with a doublet at δ 4.98. The usual methoxy group was in place and attached to a carbon atom at δ 177.2, part of a system that comprised a carbonyl at δ 195.6 and a methine at δ 101.5 (attached proton as a sharp doublet at δ 5.34 and $J = 1.1$ Hz). All those features fit into the flat structure of 5″-dihydrodichrostachine C. A NOESY experiment gave further stereochemical information: decalin *cis* junction as a consequence of NOEs between chromone H-3′ and decalin H-5″, -6″, -12, -15 (very weak correlation between 3′ and 6″, much stronger between H-3′ and H-15). None of these correlations allowed determination of the C-5″ configuration, and the 4 Hz coupling between H-5″ and H-6″ was consistent with *cis* axial−equatorial or *trans* equatorial−equatorial orientations of these protons. In the labdane rings, correlations were observed between H-5, H-7, and H-9, confirming the all-axial position of these atoms in a *trans*-decalin arrangement.

Dichrostachine P (**16**) displayed a quasimolecular ion at *m*/*z* 573 in the negative mode, corresponding to a $C_{35}H_{41}O_7$ composition. The mass discrepancy arose from the flavonoid part since the RDA fragmentation yielded an ion at *m*/*z* 285 instead of 313. It is worth noting that **15** and **16** were the sole dichrostachines for which the RDA fragmentation was observed in the negative and positive modes (sodium adducts at *m*/*z* 339 and 309). The NMR spectra showed that **16** had a different B ring flavonoid part, and the COSY experiment enabled the determination of the functionalities present on this ring starting from H-14, which led to CH_2-15 and then to H-6″ (br t). H-5″ resonated as a broad singlet at δ 4.89 ($W_{1/2} = 5$ Hz), which coupled with H-6″, thus confirming the position of an alcohol function at C-5. There was also a disubstituted double bond on this ring, part of an enone with a downfield doublet of doublets at δ 6.89 coupling with another doublet at δ 5.98 ($J = 10$ Hz). In analogy with the structure of **15**, a proposal for **16** was that of a compound with a ketone at C-2″, a C-3″−C-4″ double bond, and a C-5″ alcohol function. This product likely arose from the following sequence of events: 1,2 reduction of the C-5″ carbonyl followed by 1,4 reduction and β-elimination of the methoxy group. This hypothesis explained most of the NMR data, but several facts did not quite fit: first, there was no coupling between H-5″ and H-4″, but there was coupling between the alleged H-4″ and H-6″; second, there was a NOESY correlation between H-12 and the same H-4″! These data were best accommodated in a structure in which there was a 1,3 ketone transposition, i.e., C-4″ ketone and C-2″−C-3″ double bond. With this assignment the signal for H-4″ became H-2″, the absence of coupling between H-5″ and the double-bond protons was due to the carbonyl, and the observed coupling between H-6″ and H-2″ was a simple long-range *W* coupling.

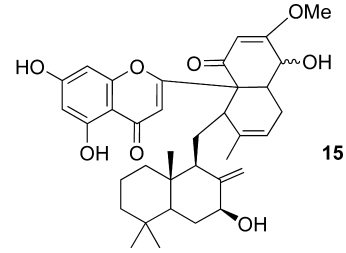

15

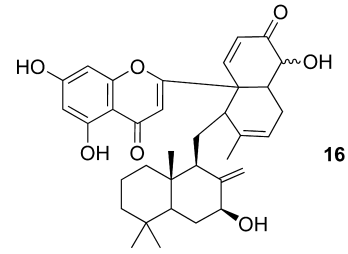

16

During the first round of structural elucidations, compound **17**, named dichrostachine Q, was assigned the structure of 11-hydroxydichrostachine C. It was an isomer of compounds **1** and **2** with a quasimolecular ion at *m*/*z* 617 in the negative mode and an RDA fragment at *m*/*z* 313. All the NMR signals fitted into the proposed structure with appropriate chemical shifts and reasonable coupling constants. Substitution at C-11 was evidenced by the downfield shifts of H-11 (double doublet at δ 4.37) and of C-10 and C-12. Subtle differences were, however, found for some

particular signals; for example, the ring junction proton H-6″ was not a triplet anymore but a singlet. Typically, dichrostachines displayed H-6″ couplings with both allylic CH_2-15, which were clearly identified through their coupling with H-14 and the higher frequency H-15 usually appearing as a doublet of doublets of quintets (large geminal and vicinal coupling, smaller long-range coupling with CH_3-16 and H-12). In compound **17** however, it appeared as a broad doublet, while its geminal upfield proton overlapped with other signals, precluding any analysis, but the COSY experiment did not show any interaction between the CH_2-15 and H-6. On the other hand, the COSY experiment showed a clear correlation between H-12 and H-6″, which did not fit the regular structure but perfectly matched a structure in which the chromone ring was at the opposite edge of the decalin ring junction. So far, dichrostachine Q is the only molecule in which the arrangement of the labdane and of the flavonoid is different. There is high probability that the change of regioselectivity of the Diels−Alder reaction finds its origin in the presence of the alcohol function at C-11, either for electronic or for steric reasons. In this regard, it is worth noting that the C-11 alcohol function could not stay free but was engaged into a hemiketal with the carbonyl C-5″ (δ_C 95).

The last of the dichrostachines, dichrostachine R (**18**), was characterized by a very strong UV absorption at 206 nm, shoulders at 225 and 275, and a band at 360 nm, and a much simpler IR carbonyl pattern consisting of a single sharp band at 1730 cm^{-1}. The mass spectrum showed a quasimolecular ion at *m*/*z* 571 ($C_{35}H_{39}O_7$) in the negative mode and a fragment at *m*/*z* 309, which was analyzed for $C_{17}H_9O_6$. The labdane moiety was identified by means of the usual ^1H and ^{13}C 1D and 2D NMR experiments, but contrary to the other compounds, identification led to a 7-hydroxy-drimane that was substituted by a trisubstituted olefin moiety bearing a methyl group and the equivalent of the flavonoid part. Despite a composition corresponding to the addition of a diterpene to a flavonoid, the Diels−Alder fragmentation was not observed. The ^1H NMR spectrum of the upper aromatic part of the molecule was characterized by two low-field AX systems, one with an *o*-coupling (8.3 Hz) and the other with *m*-coupling of the flavonoid A ring. Three further coupled protons were located in the middle of the spectrum, featuring a $CHCH_2$ fragment. The HMBC experiment allowed linking of this two-carbon unit to the trisubstituted double bond and to the other aromatic carbon atoms. Examination of the HMBC correlation identified a naphtho-benzopyran ring system instead of the usual chromone-decalin arrangement. Attachment of the drimane moiety on one of the methylene carbons was secured by the observation of correlations between the methylene protons and the B-ring carbon (flavonoid numbering) and between the methine and the C-ring carbon atoms.

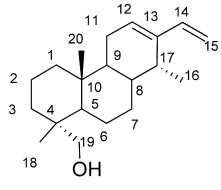

19

The last new compound (**19**) was an isomer of raimonol, which also contained a diene system (UV at λ_{max} 234 nm) but with no methyl substituent present. HMBC and HMQC experiments allowed identification of its skeleton as a cassane with a hydroxymethylene system at C-4 and CH_3-16 as a doublet (J = 7 Hz) at δ 0.97 in a α axial position because of its high-field carbon resonance (δ 14.4).

The candidate for the non-terpenoid part in the Diels−Alder reaction could be a flavonoid-derived quinone such as **20**. The main problem with this hypothesis is that quinones derived from flavonoids have not been described as natural products, despite the

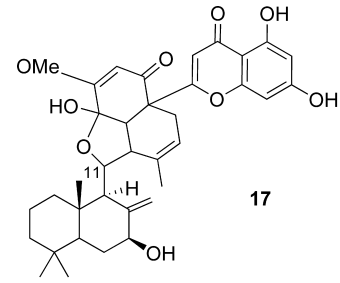

17

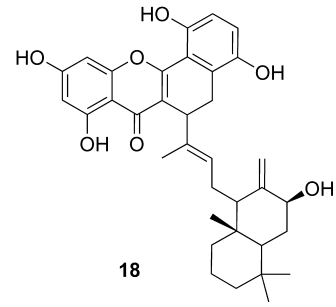

18

fact that some are stable and can be synthetically prepared (*vide infra*). Dihydroquinones corresponding to **20** are rare, and their presence in the *Dichrostachys* extracts was limited to rhamnitrin[9] and myricitrin 3-*O*-α-L-rhamnoside,[10] quercetin derivatives with the interesting feature of *O*-methylation at C-7. No flavonoid with *p*-dihydroxy substitution in ring B could be isolated. This absence raised the interesting question of oxidations in the B ring of flavonoids. Some plants, ferns in particular, are able to oxidize the B ring of flavonoids, and although originally discovered in the early 1980s,[11] the molecules were largely unnoticed until the recent discovery of their cytotoxic activity, the main bioactive compound being protoapigenone.[12] It is most probable that *Dichrostachys* possesses the enzymatic system able to synthesize the flavonoid quinone, which is then processed into Diels−Alder adducts presumably via another enzymatic system to account for the high regio- and stereoselectivities of the reactions.

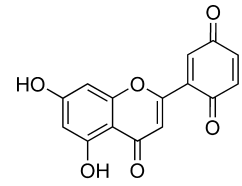

20

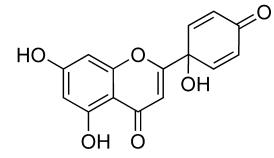

protoapigenone

Labdanetrienes are numerous (80 entries in the Dictionary of Natural Products), and despite their high reactivity, there are no reported intermolecular Diels−Alder reactions with these compounds.[13] In the natural product area however, there are at least two examples of compounds formed along this principle: in *Xylopia* species, with a kaurane (dienophile was an enone and the diene was a 16−13, 14−15 labdadiene),[14] and in the rare eunicellan diterpene of *Vellozia magdalenae* (diene is 12−13, 14−15).[15] Given the originality of the molecules and their potentially interesting biological activity, it was decided to briefly explore the feasibility of such a reaction. A separate paper[16] gave a preliminary account of this work and described the fact that flavonoid quinones such as

Scheme 1. Reaction of Methyl Communate with Flavoquinone **21**

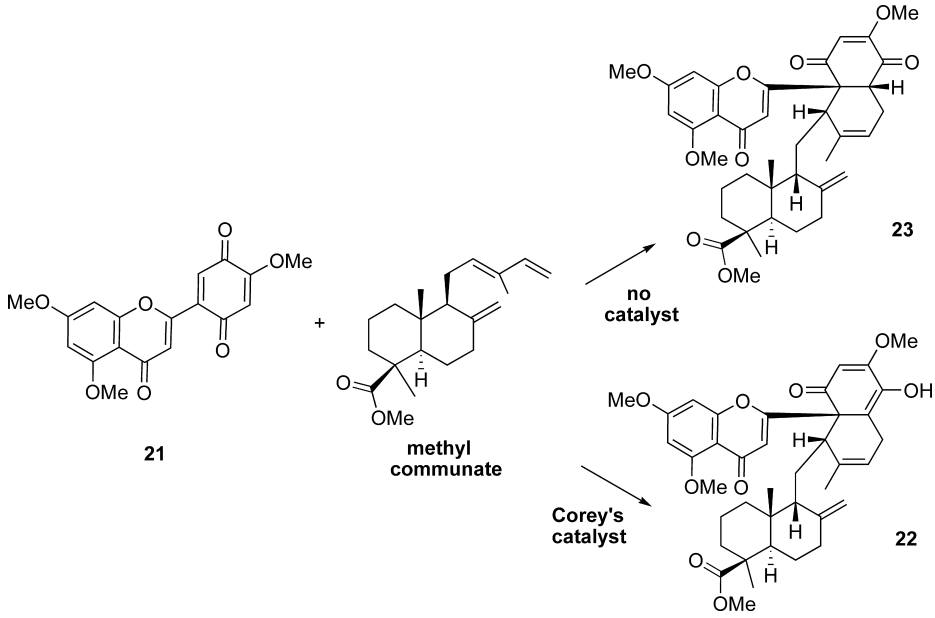

21, made according to a literature procedure,[17] were very reactive dienophiles that yielded Diels−Alder adducts under mild conditions, in the absence of a catalyst, and with a variety of dienes. The labdane diene used as a model was *trans*-methyl communate, prepared from *trans* communic acid isolated from *Cupressus sempervirens.*[18] In a first series of experiments, the reaction was catalyzed with diverse Lewis acids, just provoking decomposition, but one of Corey's chiral reagents, 3,3-diphenyl-1-*o*-toluyltetrahydropyrrolo[1,2-*c*][1,3,2]oxazaborolidinium,[19] gave a moderate yield of a compound (**22**) whose spectral properties were compatible with those of an adduct. Surprisingly, with no catalyst, the reaction proceeded equally smoothly in dichloromethane at room temperature to give an adduct (**23**) possessing similar but not identical spectral properties (Scheme 1). Compound **23** was stable enough to allow NMR characterization, but it slowly decomposed in $CDCl_3$, as the *O*-methyl derivative **13** did. The product obtained under Corey's conditions, **22**, was purified, and both compounds were shown to be isomers by mass spectrometry (*m/z* 658 for a $C_{39}H_{46}O_9$ composition). The most striking dissimilarities between their ^1H NMR spectra were found for CH_2-15, which, in **23**, as in the natural products, displayed a complex pattern of couplings with H-14 and H-6″ and, in **22**, appeared as an AX system broadened by coupling with H-14. Clearly H-6″ was missing and compound **22** was demonstrated to be the enol form of **23** by the HMBC experiment. The regio and stereo outcomes of the reaction were determined by analysis of the correlations observed in the COSY, HMBC, and ROESY experiments: the analysis started with C-1″ identified by a correlation with H-3′, which showed a coupling with H-11, thus settling the question of the regioselectivity of the addition. This was further confirmed by the observation of couplings between CH_2-15 and C-6″ in **22**. *Cis* ring junction for the decalin in **23** was established by observation of NOEs between H-3′ and H-6. It is not clear if the difference in the course of the reactions was due to Corey's reagent or to the process of purification in the presence of traces of the catalyst and related substances. It is worth noting however that the condensation proceeded under very mild conditions with high regio- and stereoselectivities, and it is not known whether Nature uses an enzyme catalyst or not.

At this point, the relative and absolute configurations of the natural and hemisynthetic compounds still needed to be defined. The available data were NOEs and some very particular chemical shifts that witnessed long-range interactions. Molecular modeling by "quenching molecular dynamics" was used to build models from which distances and NOEs could be assessed and energies calculated. The first compounds to be investigated were the synthetic compounds, and although it was not possible to interconvert **22** and **23** because of extensive decomposition, the question of the isolation of a ketone and of its enol counterpart under similar conditions was submitted to calculations. In each case, four diastereoisomeric ketones and enols were simulated (Figure 1), and it was found that for one pair of those, **22B/23B**, the global minimum energy difference was very low (19 vs 19.2 kcal/mol). The near image corresponding pair **22C/23C** also displayed one of the lowest energy differences, but it was significantly higher (2.2 vs 0.2 kcal/mol). This could explain why it was possible to isolate from the same reaction either the ketone or the enol in the presence of a Lewis acid catalyst. The models also offered an explanation for the NOEs with observation of short distances between H-3′ and H-12 and CH_3-16; the NOE between H-6″ and H-3′ required a rotation around the C-1″−C-2′ bond, which was allowed by the low energy barrier. Regarding the relative configuration of the two halves of the molecules, a clue was obtained by the observation of unusually shielded signals for CH_3-20 at δ 0.4 in **22** and 0.37 in **23** (δ 0.57 in methyl communate). Examination of the molecular models showed that CH_3-20 lay in the axis of the double bond of the vinylogous ester function at a distance of ca. 4 Å in the preferred models **22B/23B**. Given the known absolute configuration of communic acid, the configuration of **23** therefore was 4*R*, 5*R*, 9*S*, 10*R*, 12*S*, 1″*S*, 6″*R*.

In constrast to the semisynthetic compounds, the natural products displayed NOEs between H-6″ and H-11, and recourse to the models was not necessary to demonstrate that the series had opposite configuration at C-12. Conformation was thus as in model **A**, and the question of the relative configuration of the decalin and of the labdane could be settled by the observation of the extreme shielding of H-5 in compounds **2**, **3**, **15**, and **16** (δ < 0.3). In model **A**, the labdane was stacked on the flavonoid and a distance of 3.2 Å was measured between H-5 and the center of the aromatic ring, thus accounting for a strong shielding due to the ring current effect. In the series, the chemical shift of H-5 spans from δ 0.18 to 1.5, reflecting not a configurational change but differences in populations of conformers. Assuming that all natural compounds had the absolute configuration of raimonol, their configuration is 4*R*, 5*R*, 9*S*, 10*R*, 12*R*, 1″*S*, 6″*R*. A simple explanation for the difference in the stereochemical outcome of the reactions (chemistry vs Nature) is probably to be found in the difference of configuration of the 12−13 trisubstituted double bond in the labdane trienes, and it

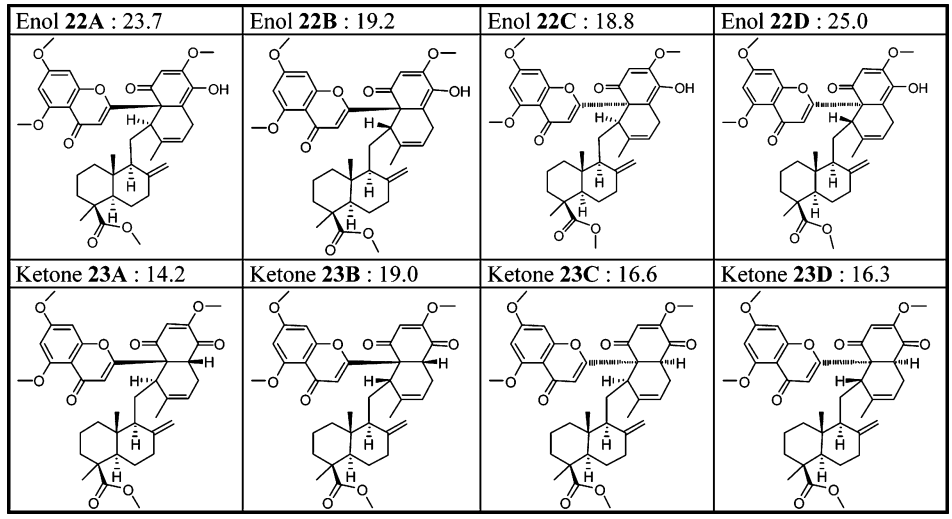

Figure 1. Energy minimization of diastereoisomeric enols **22** and ketones **23**.

Table 3. *In Vitro* PFTase Inhibition of Dichrostachines A−H, L, M, O, P, and R

compound	IC_{50} (μM)
1	10
2	40
3	5.7
4	86
5	40
7	17
8	1.8
12	3.2
13	3
15	25
16	7
18	37
SCH-66336	0.1

would have been interesting to run the reaction with raimonol instead of the methyl communate to settle this point.

The PFTase enzyme inhibition was measured for dichrostachines A to H, L, M, O, P, and R. The IC_{50} values, identified as the dichrostachine concentrations inhibiting 50% of the PFTase activity (Table 3), ranged from 1.8 μM for dichrostachine H to 90 μM for dichrostachine D, indicating that both active and nonactive dichrostachines could be detected in the screening process. Compound **1** was not the most active compound isolated from the root bark, and minor compound **3** showed a slightly better activity, thus demonstrating the difficulties of bioassay-guided fractionation when several active compounds are present at different concentrations. Two of the two most active compounds, **13** and **14**, were also the most reactive (conjugated enones), and their higher activity was most probably due to nonspecific interaction with the enzyme via Michael conjugation. These two compounds were also the most cytotoxic (3.1 and 2.8 μM, while all others had cytotoxicity > 10 μM), which pointed to other possible modes of action. In the nonreactive compounds, it seemed that activity was lowered by hydroxylation at C-2, and the most active of those was aldehyde **8** (dichrostachine H), with hydroxymethyl (**1**) and methyl (**3**) half an order of magnitude less potent than **8**. Despite the fact that the most active compound, dichrostachine H, was only 20 times less potent than the reference compound, SCH-66336, a molecule presenting a strong inhibitory effect on tumor growth,[20] the complexity of the purification, and the tremendous efforts necessary to chemically improve the activity brought this program to a halt.

Experimental Section

General Experimental Procedures. Optical rotations were measured on a Perkin-Elmer 341 automatic polarimeter. UV spectra were obtained in MeOH using a UV MC^2 Safas spectrophotometer. An FT-IR Bruker Tensor 27 spectrophotometer was used for scanning IR spectroscopy. The NMR spectra were recorded on a Bruker Avance equipped with a ^{13}C cryoprobe at 500 MHz for ^1H and 125 MHz for ^{13}C; 2D experiments were performed using standard Bruker programs. The ESIMS and MSMS were performed using a Bruker Esquire-LC ion trap mass spectrometer. The samples were introduced by infusion in MeOH solution. HRESIMS were obtained on a Bruker MicroTOF. TLC was carried out on precoated silica gel $60F_{254}$ (Merck) with $CHCl_3$−MeOH (90:10), and spots were visualized by spraying with 3% H_2SO_4 + 1% vanillin. Column chromatography (CC) was carried out on Kieselgel (40−60 μm) with a binary gradient elution (solvent A, CH_2Cl_2; solvent B, MeOH) or LiChroprep RP-18 (15−25 μm) with a binary gradient elution (solvent A, H_2O−0.1% HOAc; solvent B, MeCN−0.1% HOAc). Analytical HPLC was performed on a Merck-Hitachi apparatus equipped with an L-7200 automated sample injector, an L-7100 pump, an L-7450 diode array detector, a D-7000 interface, and Lachrom HSM software. A prepacked C_{18} reversed-phase column (Lichrospher 100 RP18, 4 × 125 mm, 5 μm) was used for analytical HPLC with a binary gradient elution (solvent A, H_2O−0.1% HOAc; solvent B, MeCN−0.1% HOAc) and a flow rate of 1 mL min^{-1}. Semipreparative HPLC was performed on an apparatus equipped with a Waters 600 pump, a Waters 2487 Dual λ absorbance detector, and Empower software. A prepacked C_{18} reversed-phase column (Hibar-Lichrospher 100 RP18, 25 × 250 mm, 5 μm) was used for semipreparative HPLC with a binary gradient elution (solvent A, H_2O−0.1% HOAc; solvent B, MeCN−0.1% HOAc) and a flow rate of 30 mL min^{-1}, and the chromatogram was monitored at 235 and 255 nm.

Plant Material. The plant material was collected by one of us (C.D.) at Menkao, Bateke Plateau, Democratic Republic of Congo (former Zaire), in October 1971; identification was performed by Dr. H. Breyne and found identical with authentic sample HB No. 383, deposited in the Herbarium of the Royal Garden of Brussels (Belgium).

Extraction and Isolation. The dried root bark (300 g) of *D. cinerea* was extracted at room temperature with EtOAc (2 L) overnight. After filtration, the extract was concentrated under reduced pressure and the residue (5.45 g) was partitioned between MeOH (2.77 g) and hexanes (2.40 g). The MeOH fraction was subjected to silica gel column chromatography (120 g, 3.5 × 23 cm) using a gradient of CH_2Cl_2−MeOH (100 to 85:15) for 90 min to give 180 fractions of 15 mL. All the fractions were analyzed by TLC on silica gel using the solvent mixture $CHCl_3$−MeOH (90:10) and pooled according to TLC into 11 fractions (R1−R11). Fraction R1 (48 mg), eluted with 100% CH_2Cl_2, was purified by semipreparative RP 18 chromatography, eluting with a linear gradient (65 to 90% B) for 40 min, to give 1.4 mg of raimonol (0.0005%) and 2.3 mg of **19** (0.0008%). Fraction R4 (315 mg) was further purified by semipreparative RP 18 chromatography, eluting with a linear gradient (60 to 100% B) for 40 min, to give after repeated HPLC purification **2** (7.0 mg, 0.0023%), **3** (9.4 mg, 0.0031%), **6** (3.3 mg, 0.0011%), and **7** (11.9 mg, 0.0040%). Fraction R6 (370 mg) and fraction R8 (152 mg) were purified by semipreparative RP 18

3D models for the synthetic (top) and natural (bottom) isomers

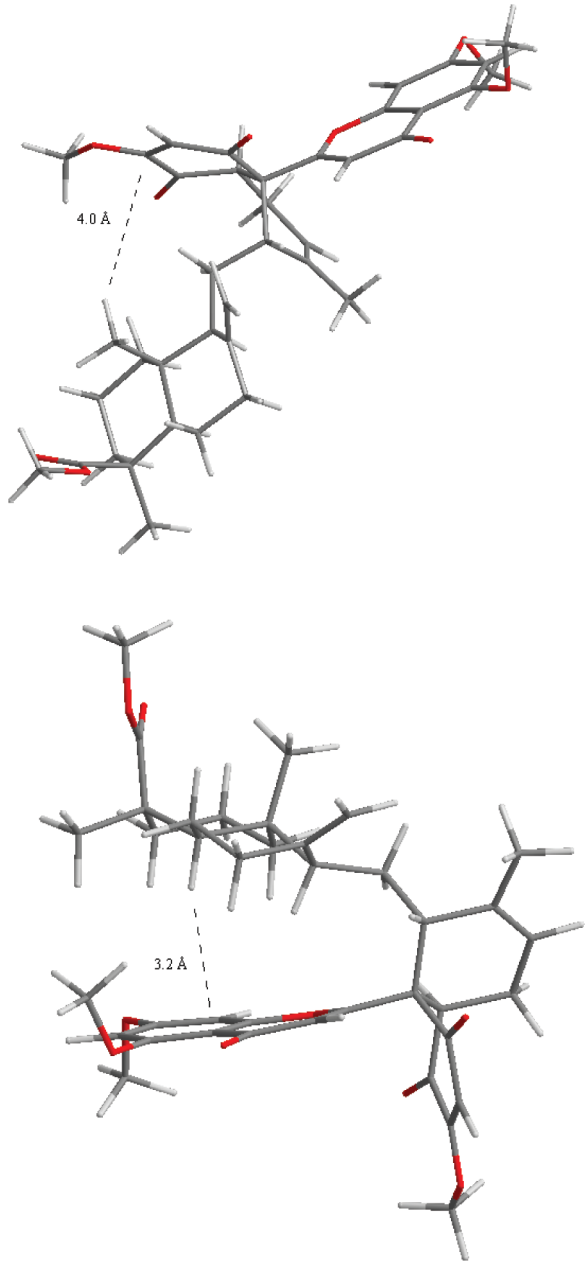

chromatography, eluting with 45% B, to give **1** (49.9 mg, 0.0166%) and **5** (6.8 mg, 0.0023%).

The second batch of roots (1 kg) was treated as above, and after the first column chromatography, six fractions were obtained (RB1−RB6). Fraction RB2 (4.8 g) was subjected to C_{18} (15−25 μm) column chromatography (120 g, 3.5 × 23 cm) with a linear gradient (40 to 100% B) to give 76 fractions of 100 mL, which were analyzed by HPLC over C_{18} with the gradient elution program 40 to 70% B for 25 min and pooled into 24 fractions. These fractions were further purified by crystallization in MeOH to yield **2** (120 mg, 0.012%), **11** (7 mg, 0.0007%), **12** (35 mg, 0.0035%), **13** (14 mg, 0.0014%), and **4** (40 mg, 0.004% dry) or by semipreparative RP 18 chromatography, with a linear gradient (10 to 100% B) for 37.5 min, to yield **1** (8 mg, 0.0008%), **10** (3 mg, 0.0003%), **14** (3 mg 0.0003%), **9** (3.1 mg, 0.0003%), and **8** (6 mg, 0.0006%). Fraction RB3 (4.15 g) was subjected to C18 column chromatography (430 g, 7 × 46 cm) eluting with 40% B, and from the 49 fractions of 100 mL were obtained **4** (37 mg, 0.0037%), **2** (130 mg, 0.013%), and **5** (100 mg, 0.01%).

In a similar fashion, the stem bark (500 g) yielded 7.43 and 4.56 g of MeOH and hexanes fractions, respectively. The MeOH fraction was processed as above into eight fractions. Fractions B1−B2 (122 and 62 mg) gave raimonol (8.6 mg, 0.0017%) after semipreparative RP 18 chromatography and repeated HPLC. Fractions B6−B7 (156 and 731 mg) were subjected to C_{18} (15−25 μm) column chromatography (120 g, 3.5 × 23 cm) with a linear gradient (40 to 90% B) for 80 min to give after analysis (TLC and analytical HPLC) five fractions (B9−B13). Fraction B9 (568 mg) was purified by semipreparative RP 18 chromatography, eluting with 40% B, to give **2** (52.7 mg, 0.0105%). Fraction B10 (219 mg) was purified by semipreparative RP 18 chromatography, with a linear gradient (40 to 60% B) for 75 min, to give **15** (9.8 mg, 0.0020% dry weight), **16** (16.3 mg, 0.0033%), **17** (2.9 mg, 0.0006%), and **2** (6.7 mg, 0.0013%). Fraction B12 (134 mg) was purified by semipreparative RP 18 chromatography, with a linear gradient (50 to 75% B) for 40 min, to give **3** (6.1 mg, 0.0012%). Fraction B13 (222 mg) was purified by semipreparative RP 18 chromatography, with a linear gradient (60 to 75% B) for 50 min, to give **18** (3.5 mg, 0.0007%).

The leaves (500 g) of *D. cinerea* were treated in a similar fashion to yield MeOH (2.69 g) and hexanes (5.35 g) fractions. The MeOH fraction was subjected to silica gel column chromatography (120 g, 3.5 × 23 cm) using a gradient of CH_2Cl_2−MeOH (100 to 85:15) for 90 min to give 180 fractions of 15 mL. The fractions were analyzed by TLC on silica gel using the solvent mixture $CHCl_3$−MeOH (90:10) to obtain 10 fractions (L1−L10). Fraction L9 (90 mg) was purified by semipreparative RP 18 chromatography, eluting with a linear gradient (20 to 35% B) for 50 min, to give myricitrin 3-*O*-α-L-rhamnoside (1.6 mg, 0.0003%).

Dichrostachine A (1): yellow gum, $[\alpha]^{20}_D$ −51 (*c* 0.27, MeOH); UV (MeOH) λ_{max} (log ϵ) 210 (4.16), 264 (4.06), 330 sh (3.47) nm; IR ν_{max} (film) 3435, 2928, 1710, 1651, 1609, 1574, 1165 cm^{-1}; ^{1}H NMR ($CDCl_3$, 500 MHz) δ 12.5 (OH-5′), 6.42 (1H, br s, H-8′), 6.30 (1H, br s, H-6′), 6.17 (1H, s, H-3′), 5.81 (1H, s, H-3″), 5.26, 4.84 (each 1H, br s, H-17), 5.24 (1H, br s, H-14), 3.81 (1H, t, J = 9 Hz, H-6″), 3.73 (3H, s, OMe), 3.23 (1H, m, H-7), 3.2 (1H, m, H-12), 3.18 (1H, d, J = 11 Hz, H-19), 2.94 (1H, d, J = 11 Hz, H-19), 2.62 (1H, m, H-15), 2.19 (1H, m, H-15), 1.9 (3H, br s, H-16), 0.67 (1H, d, J = 13 Hz, H-5), 0.61 (3H, s, H-18), 0.58 (3H, s, H-20); ^{1}H NMR (CD_3OD, 500 MHz) δ 6.14 (1H, br s, H-8′), 6.12 (1H, br s, H-6′), 5.99 (1H, br s, H-3′), 5.96 (1H, s, H-3″), 5.25 (2H, br s, H-14, H-17), 4.85 (1H, br s, H-17), 3.84 (1H, t, J = 11 Hz, H-6″), 3.74 (3H, s, OMe), 3.39 (1H, m, H-7), 3.09 (1H, dd, J = 6.5, 5 Hz, H-12), 3.00 (2H, m, H-19), 2.62 (1H, ddq, J = 18, 9, 1 Hz, H-15), 2.20 (1H, ddm, J = 18 Hz, H-15), 1.86 (3H, br s, H-16), 0.66 (3H, s, H-18), 0.59 (3H, s, H-20); ^{1}H NMR (CD_3CN, 500 MHz) δ 12.44 (OH-5′), 6.23 (1H, br s, H-8′), 6.22 (1H, br s, H-6′), 5.99 (1H, br s, H-3′), 5.84 (1H, s, H-3″), 5.23 (1H, m, H-14), 5.17, 4.80 (each 1H, s, H-17), 3.80 (1H, t, J = 9 Hz, H-6″), 3.67 (3H, s, OMe), 3.25 (1H, dd, J = 10, 5 Hz, H-7), 3.05 (1H, dd, J = 7.5, 4.5 Hz, H-12), 2.99 (1H, d, J = 10 Hz, H-19), 2.82 (1H, d, J = 10 Hz, H-19), 2.53 (1H, ddq, J = 18, 9, 1 Hz, H-15), 2.12 (1H, m, H-15), 1.82 (3H, d, J = 1.5 Hz, H-16), 1.64 (1H, ddd, J = 12, 5.3, 2.3, Hz, H-6eq), 1.47 (1H, dt, J = 12, 3 Hz, H-1eq), 1.11 (2H, m, 2H-3), 1.06 (1H, dd, J = 10, 3.3 Hz, H-9),), 0.96 (1H, q, J = 12 Hz, H-6ax), 0.74 (1H, dd, J = 12, 2.5 Hz, H-5), 0.58 (3H, s, H-18), 0.53 (3H, s, H-20); ^{13}C NMR, see Table 1; HRMS *m*/*z* 617.2761 (calcd for $C_{36}H_{41}O_9$ 617.2756); *m*/*z* 313.0349 (calcd for $C_{19}H_9O_7$ 313.0354).

Dichrostachine B (2): white solid, $[\alpha]^{20}_D$ −161 (*c* 0.12, MeOH); UV (MeOH) λ_{max} (log ϵ) 212 (4.02), 262 (3.99), 330 (3.47) nm; IR ν_{max} (film) 3390, 1715, 1650, 1614, 1354, 1021, 756 cm^{-1}; ^{1}H NMR ($CD_3OD/CDCl_3$, 9:1, 500 MHz) δ 6.40 (1H, br s, H-8′), 6.26 (1H, d, J = 1.4 Hz, H-6′), 6.08 (1H, br s, H-3′), 5.99 (1H, s, H-3″), 5.31, 4.90 (each 1H, s, H-17), 5.29 (1H, br s, H-14), 3.91 (1H, t, J = 9 Hz, H-6″), 3.76 (3H, s, OMe), 3.73 (1H, m, H-2), 3.20 (1H, dd, J = 11, 5 Hz, H-12), 3.17 (1H, d, J = 10 Hz, H-7), 2.61 (1H, dd, J = 19, 9 Hz, H-15), 2.23 (1H, dd, J = 19, 8.8 Hz, H-15), 1.91 (3H, br s, H-16), 1.71 (1H, m, H-6eq), 1.03 (1H, q, J = 12 Hz, H-6ax), 0.74 (3H, s, H-18), 0.68 (3H, s, H-19), 0.62 (3H, s, H-20), 0.18 (1H, d, J = 12 Hz, H-5); ^{13}C NMR, see Table 1; HRMS *m*/*z* 617.2760 (calcd for $C_{36}H_{41}O_9$ 617.2756).

Dichrostachine C (3): white gum, $[\alpha]^{20}_D$ −223 (*c* 0.17, MeOH); UV (MeOH) λ_{max} (log ϵ) 210 (4.16), 258 (4.08), 325 sh (3.47) nm; IR ν_{max} (film) 3395, 1715, 1655, 1603, 1190, 1170 cm^{-1}; ^{1}H NMR (CD_3OD, 500 MHz) δ 6.32 (1H, d, J = 2 Hz, H-8′), 6.25 (1H, d, J = 2 Hz, H-6′), 6.07 (1H, br s, H-3′), 6.01 (1H, s, H-3″), 5.29 (1H, br s, H-14), 5.28, 4.88 (each 1H, s, H-17), 3.87 (1H, t, J = 9 Hz, H-6″),

3.76 (3H, s, OMe), 3.29 (1H, dd, J = 11, 5 Hz, H-7), 3.14 (1H, dd, J = 8, 2 Hz, H-12), 2.61 (1H, ddq, J = 19, 9, 1.5 Hz, H-15), 2.21 (1H, dd, J = 19, 9 Hz, H-15), 1.89 (3H, d, J = 1.5 Hz, H-16), 1.75 (1H, ddd, J = 12, 5, 2.3 Hz, H-6eq), 1.07 (1H, q, J = 12 Hz, H-6ax), 0.71 (3H, s, H-18), 0.66 (3H, s, H-19), 0.58 (3H, s, H-20), 0.29 (1H, d, J = 12 Hz, H-5); ^{13}C NMR, see Table 1; HRMS *m/z* 601.2810 (calcd for $C_{36}H_{41}O_8$ 601.2807).

Dichrostachine D (4): white solid, $[\alpha]^{20}_D$ −176 (*c* 0.225, MeOH/$CHCl_3$, 6:4); UV (MeOH) λ_{max} (log ϵ) 210 (4.14), 274 (3.99), 326 (3.78) nm; IR ν_{max} (film) 3272, 1715, 1640, 1605, 1014 cm^{-1}; ^{1}H NMR ($CD_3OD/CDCl_3$, 9:1, 500 MHz) δ 6.33 (1H, s, H-3′), 6.23 (1H, d, J = 2.1 Hz, H-8′), 6.2 (1H, d, J = 2.1 Hz, H-6′), 5.86 (1H, s, H-3″), 5.25 (1H, dt, J = 5, 1.8 Hz, H-14), 5.23 (1H, d, J = 1.5 Hz, H-17), 4.83 (1H, s, H-17), 4.4 (1H, dd, J = 11.5, 5.2 Hz, H-7), 3.81 (1H, dd, J = 10.5, 6.5 Hz, H-6″), 3.76 (3H, s, OMe), 3.57 (1H, tt, J = 11.5, 4 Hz, H-2), 3.46 (1H, dd, J = 10, 2.3 Hz, H-12), 2.78 (1H, ddq, J = 19, 10.5, 2 Hz, H-15), 2.14 (1H, dt, J = 19, 7 Hz, H-15), 1.93 (1H, ddd, J = 12, 5.1, 2.5 Hz, H-6eq), 1.9 (1H, dd, J = 14.4, 10 Hz, H-11), 1.85 (1H, dd, J = 13, 2.7 Hz, H-5), 1.82 (3H, br s, H-16), 1.69 (1H, dd, J = 14.4, 2.5 Hz, H-11), 1.61 (1H, dd, J = 12.5, 2.4 Hz, H-3), 1.27 (ddd, J = 11.3, 3, 1.5 Hz, H-1eq), 1.11 (1H, t, J = 11.5 Hz, H-1ax), 1.06 (1H, t, J = 12 Hz, H-6ax), 1.02 (1H, t, J = 12 Hz, H-3ax), 0.92 (3H, s, H-19), 0.77 (3H, s, H-18), 0.65 (3H, s, H-20); ^{13}C NMR, see Table 1; HRMS 633.2698 *m/z* (calcd for $C_{36}H_{41}O_{10}$ 633.2705).

Dichrostachine E (5): yellow gum, $[\alpha]^{20}_D$ −154 (*c* 0.083, MeOH); UV (MeOH) λ_{max} (log ϵ) 208 (3.93), 256 (3.6), 330 sh (3) nm; IR ν_{max} (film) 3285, 1718, 1650 cm^{-1}; ^{1}H NMR ($CD_3OD/CDCl_3$, 9:1, 500 MHz) δ 6.31 (1H, br s, H-8′), 6.26 (1H, br s, H-6′), 6.11 (1H, s, H-3′), 5.97 (1H, s, H-3″), 5.27 (2H, br s, H-14, H-17), 4.8 (1H, s, H-17), 3.86 (1H, t, J = 8.8 Hz, H-6″), 3.76 (3H, s, OMe), 3.41 (1H, dd, J = 12, 6 Hz, H-7), 3.14 (1H, t, J = 6 Hz, H-12), 2.63 (1H, br dd, J = 18, 8.5 Hz, H-15), 2.23 (1H, br d, J = 19 Hz, H-15), 1.88 (3H, br s, H-16), 1.60 (2H, t, J = 6 Hz, H-11), 0.99 (3H, s, H-18), 0.59 (3H, s, H-20); ^{13}C NMR, see Table 1; HRMS 631.2544 *m/z* (calcd for $C_{36}H_{39}O_{10}$ 631.2549).

Dichrostachine F (6): white, amorphous solid, $[\alpha]^{20}_D$ −175 (*c* 0.008, MeOH); UV (MeOH) λ_{max} (log ϵ) 210 (3.84), 250 (3.54) nm; IR ν_{max} (film) 3378, 1640 cm^{-1}; ^{1}H NMR (CD_3OD, 500 MHz) δ 6.37 (1H, br d, J = 1.8 Hz, H-8′), 6.25 (1H, s, H-3′), 6.21 (1H, br d, J = 1.8 Hz, H-6′), 5.99 (1H, s, H-3″), 5.36 (1H, br s, $W_{1/2}$ = 6 Hz, H-14), 3.87 (1H, dd, J = 10, 8 Hz, H-6″), 3.77 (3H, s, OMe), 3.7 (1H, m, H-2), 3.52 (1H, dd, J = 12, 3 Hz, H-12), 2.76 (1H, ddq, J = 19, 10, 2 Hz, H-15), 2.15 (1H, br d, J = 19 Hz, H-15), 2.01 (3H, br s, H-16), 1.79 (1H, dt, J = 13, 3 Hz, H-7), 1.47 (1H, d, J = 5.5 Hz, H-9), 1.01 (3H, s, H-17), 0.92 (3H, s, H-19), 0.87 (1H, d, J = 10.5 Hz, H-5), 0.8 (3H, s, H-18), 0.6 (3H, s, H-20); ^{13}C NMR, see Table 1; HRMS 619.2900 *m/z* (calcd for $C_{36}H_{43}O_9$ 619.2913).

Dichrostachine G (7): white solid, $[\alpha]^{20}_D$ −87 (*c* 0.108, MeOH); UV (MeOH) λ_{max} (log ϵ) 212 (4.29), 256 (4.24) nm; IR ν_{max} (film) 3394, 1715, 1650, 1607, 1021 cm^{-1}; ^{1}H NMR (CD_3OD, 500 MHz) δ 6.39 (1H, d, J = 1.8 Hz, H-8′), 6.29 (1H, s, H-3′), 6.22 (1H, d, J = 1.8 Hz, H-6′), 5.98 (1H, s, H-3″), 5.31 (1H, br s, H-14), 3.85 (1H, dd, J = 10.5, 6.5 Hz, H-6″), 3.78 (3H, s, OMe), 3.71 (1H, dd, J = 8, 2 Hz, H-12), 3.66 (1H, m, H-2), 2.85 (1H, m, H-15), 2.13 (1H, br d, J = 18 Hz, H-15), 2.01 (3H, br s, H-16), 1.96 (1H, m, H-1), 1.87 (1H, dd, J = 15.2, 9.5 Hz, H-11), 1.77 (1H, dd, J = 15.2, 2 Hz, H-11), 1.68 (4H, m, H-1, H-3, H 5, H-7), 1.52 (1H, br d, J = 12 Hz, H-6eq), 1.46 (1H, dt, J = 12, 2 Hz, H-7eq), 1.21 (3H, s, H-17), 1.08 (1H, t, J = 12 Hz, H-3ax), 0.92 (3H, s, H-19), 0.79 (3H, s, H-18), 0.68 (3H, s, H-20); ^{13}C NMR, see Table 1; HRMS *m/z* 635.2865 (calcd for $C_{36}H_{43}O_{10}$ 635.2862).

Dichrostachine H (8): yellow oil, $[\alpha]^{20}_D$ −125 (*c* 0.175, MeOH); UV (MeOH) λ_{max} (log ϵ) 210 (4.2), 258 (4.11), 330 sh (3.6) nm; IR ν_{max} (film) 3275, 1715, 1652, 1605, 1017 cm^{-1}; ^{1}H NMR ($CDCl_3$, 500 MHz) δ 8.81 (1H, s, H-19), 6.4 (1H, br s, H-8′), 6.36 (1H, br s, H-6′), 6.18 (1H, s, H-3′), 5.83 (1H, s, H-3″), 5.29 (1H, br s, H-17), 5.26 (1H, br s, H-14), 4.87 (1H, s, H-17), 3.79 (1H, m, H-6″), 3.75 (3H, s, OMe), 3.21 (2H, m, H-12, H-7), 2.62 (1H, dd, J = 19, 10 Hz, H-15), 2.2 (1H, m, H-15), 1.9 (3H, br s, H-16), 1.15 (4H, m, H-3, H-6), 0.89 (3H, s, H-18), 0.59 (3H, s, H-20); ^{13}C NMR, see Table 1; HRMS *m/z* 615.2607 (calcd for $C_{36}H_{39}O_9$ 615.2600).

Dichrostachine I (9): yellow oil, $[\alpha]^{20}_D$ −144 (*c* 0.167, MeOH); UV (MeOH) λ_{max} (log ϵ) 212 (4.28), 256 (4.16), 330 sh (3.48) nm; IR ν_{max} (film) 3283, 1650 cm^{-1} (broadband); ^{1}H NMR ($CD_3OD/CDCl_3$, 9:1, 500 MHz) δ 6.26 (1H, d, J = 2.1 Hz, H-8′), 6.22 (1H, d, J = 2.1 Hz, H-6′), 6.15 (1H, s, H-3′), 5.86 (1H, s, H-3″), 5.84 (1H, d, J = 2 Hz, H-17), 5.28 (1H, m, H-14), 5.25 (1H, br d, J = 2 Hz, H-17), 3.75 (1H, t, J = 9 Hz, H-6″), 3.74 (3H, s, OMe), 3.12 (1H, d, J = 11 Hz, H-19), 3.06 (1H, dd, J = 8, 5 Hz, H-12), 2.93 (1H, d, J = 11 Hz, H-19), 2.68 (1H, ddq, J = 19, 10, 2 Hz, H-15), 2.37 (1H, dd, J = 17.5, 4.5 Hz, H-6), 2.22 (1H, m, H-15), 2.17 (1H, dd, J = 17.5, 14 Hz, H-6), 1.92 (1H, m, H-9), 1.79 (3H, br s, H-16), 1.62 (1H, ddd, J = 15, 5, 2 Hz, H-11), 1.55 (1H, dd, J = 13.5, 4.5 Hz, H-5), 1.45 (1H, dt, J = 15, 8 Hz, H-11), 0.68 (3H, s, H-18), 0.65 (3H, s, H-20); ^{13}C NMR, see Table 2; HRMS *m/z* 615.2597 (calcd for $C_{36}H_{39}O_9$ 615.2600).

Dichrostachine J (10): white solid, $[\alpha]^{20}_D$ −178 (*c* 0.125, MeOH); UV (MeOH) λ_{max} (log ϵ) 210 (4.19), 258 (4.09), 330 sh (3.48) nm; IR ν_{max} (film) 3288, 1650 cm^{-1}; ^{1}H NMR ($CDCl_3$, 500 MHz) δ 6.38 (1H, br s, H-8′), 6.33 (1H, br s, H-6′), 6.23 (1H, s, H-3′), 5.90 (1H, d, J = 1.5 Hz, H-17), 5.83 (1H, s, H-3″), 5.32 (1H, m, H-14), 5.3 (1H, br s, H-17), 3.82 (2H, m, H-6″, H-2), 3.75 (3H, s, OMe), 3.21 (1H, t, J = 6 Hz, H-12), 2.68 (1H, m, H-15), 2.37 (1H, dd, J = 17.5, 4.6 Hz, H-6), 2.21 (1H, m, H-15), 2.11 (1H, m, H-6), 1.9 (3H, br s, H-16), 1.62 (1H, m, H-9), 0.82 (1H, m, H-5), 0.8 (3H, s, H-18), 0.77 (3H, s, H-19), 0.7 (3H, s, H-20); ^{13}C NMR, see Table 2; HRMS *m/z* 615.2584 (calcd for $C_{36}H_{39}O_9$ 615.2600).

Dichrostachine K (11): white gum, $[\alpha]^{20}_D$ −76 (*c* 0.05, MeOH); UV (MeOH) λ_{max} (log ϵ) 208 (3.87), 250 (3.6) nm; IR ν_{max} (film) 3400, 1715, 1645, 1605 cm^{-1}; ^{1}H NMR ($CD_3OD/CDCl_3$, 9:1, 500 MHz) δ 6.28 (1H, s, H-3′), 6.27 (1H, br s, H-8′), 6.21 (1H, d, J = 2 Hz, H-6′), 5.94 (1H, s, H-3″), 5.62 (1H, br s, H-17), 5.3 (1H, br s, H-17), 5.29 (1H, m, H-14), 3.83 (1H, dd, J = 10, 7.5 Hz, H-6″), 3.76 (3H, s, OMe), 3.50 (1H, dd, J = 9, 3 Hz, H-12), 2.76 (1H, m, H-15), 2.45 (1H, dd, J = 15, 2.5 Hz, H-6), 2.18 (1H, m, H-15), 2.17 (1H, m, H-6), 1.77 (3H, br s, H-16), 0.84 (3H, s, H-19) 0.82 (3H, s, H-18), 0.77 (3H, s, H-20); ^{13}C NMR, see Table 2; HRMS *m/z* 615.2602 (calcd for $C_{36}H_{39}O_9$ 615.2600).

Dichrostachine L (12): white gum, $[\alpha]^{20}_D$ −181 (*c* 0.108, MeOH); UV (MeOH) λ_{max} (log ϵ) 212 (4.32), 256 (4.23), 330 sh (3.7) nm; IR ν_{max} (film) 3335, 1650, 1605 cm^{-1}; ^{1}H NMR ($CDCl_3$, 500 MHz) δ 6.21 (1H, d, J = 2.1 Hz, H-6′), 6.15 (1H, s, H-3′), 6.14 (1H, d, J = 2.1 Hz, H-8′), 5.76 (1H, m, H-17), 5.72 (1H, s, H-3″), 5.23 (1H, m, H-14), 5.21 (1H, br s, H-17), 3.68 (3H, s, OMe), 3.61 (1H, t, J = 8.9 Hz, H-6″), 3.13 (1H, dd, J = 8, 4.5 Hz, H-12), 2.57 (1H, ddq, J = 19, 9, 2 Hz, H-15), 2.21 (1H, dd, J = 18, 4.5 Hz, H-6), 2.14 (1H, m, H-15), 2.02 (1H, m, H-6), 1.82 (3H, br s, H-16), 0.66 (3H, s, H-18) 0.63 (3H, s, H-19), 0.56 (3H, s, H-20); ^{13}C NMR, see Table 2; HRMS *m/z* 599.2641 (calcd for $C_{36}H_{39}O_8$ 599.2650).

Dichrostachine M (13): white solid, $[\alpha]^{20}_D$ −163 (*c* 0.142, MeOH); UV (MeOH) λ_{max} (log ϵ) 210 (4.27), 254 (4.16), 330 sh (3.54) nm; IR ν_{max} (film) 3380, 1716, 1655, 1604, 1162 cm^{-1}; ^{1}H NMR ($CDCl_3$, 500 MHz) δ 12.26 (1H, s, OH), 6.31 (2H, s, H-6′, H-8′), 6.21 (1H, s, H-3′), 5.81 (1H, m, H-17), 5.78 (1H, s, H-3″), 5.26 (1H, m, H-14), 5.20 (1H, br s, H-17), 3.86 (3H, s, 7′-OMe), 3.72 (3H, s, 4″-OMe), 3.71 (1H, m, H-6″), 3.15 (1H, t, J = 6.4 Hz, H-12), 2.64 (1H, ddq, J = 19, 8, 1.6 Hz, H-15), 2.28 (1H, dd, J = 18, 4.5 Hz, H-6), 2.19 (1H, m, H-15), 2.08 (1H, dd, J = 18, 14 Hz, H-6), 1.84 (3H, br s, H-16), 0.71 (3H, s, H-18), 0.68 (3H, s, H-19), 0.59 (3H, s, H-20); ($CD_3OD/CDCl_3$, 9:1, 500 MHz) δ 6.38 (1H, d, J = 2.2 Hz, H-8′), 6.32 (1H, d, J = 2.2 Hz, H-6′), 6.2 (1H, s, H-3′), 5.87 (1H, s, H-3″), 5.79 (1H, br d, J = 1.7 Hz, H-17), 5.29 (1H, m, H-14), 5.26 (1H, br d, J = 1.7 Hz, H-17), 3.87 (3H, s, 7′-OMe), 3.75 (1H, m, H-6″), 3.74 (3H, s, 4′-OMe), 3.15 (1H, t, J = 6.5 Hz, H-12), 2.66 (1H, ddq, J = 19, 8, 1.6 Hz, H-15), 2.25 (1H, dd, J = 17.7, 4.5 Hz, H-6), 2.2 (1H, m, H-15), 2.11 (1H, dd, J = 17.5, 14 Hz, H-6), 1.83 (3H, br s, H-16), 0.72 (3H, s, H-19), 0.68 (3H, s, H-18), 0.63 (3H, s, H-20); ^{13}C NMR, see Table 2; HRMS *m/z* 637.2761 (calcd for $C_{37}H_{42}O_8Na$ 637.2772).

Dichrostachine N (14): white solid, $[\alpha]^{20}_D$ −375 (*c* 0.008, MeOH); UV (MeOH) λ_{max} (log ϵ) 210 (3.74), 250 sh (3.47), 300 sh (3.3) nm; IR ν_{max} (film) 3400, 1647, 1600 cm^{-1}; ^{1}H NMR ($CD_3OD/CDCl_3$, 9:1, 500 MHz) δ 6.39 (1H, d, J = 2.2 Hz, H-8′), 6.33 (1H, s, H-3′), 6.31 (1H, d, J = 2.2 Hz, H-6′), 5.89 (1H, s, H-3″), 5.62 (1H, br s, H-17), 5.32 (1H, br s, H-17), 5.30 (1H, m, H-14), 3.86 (3H, s, 7′-OMe), 3.76 (3H, s, 4′-OMe), 3.80 (1H, m, H-6″), 3.62 (1H, m, H-2), 3.49 (1H, dd, J = 9, 2 Hz, H-12), 2.74 (1H, ddq, J = 19, 8, 1.6 Hz, H-15), 2.45 (1H, dd, J = 16, 3 Hz, H-6), 2.19 (1H, m, H-15), 2.14 (1H, dd, J = 18, 14 Hz, H-6), 1.78 (3H, br s, H-16), 0.88 (3H, s, H-19), 0.85 (3H, s, H-18), 0.80 (3H, s, H-20); ^{13}C NMR, see Table 2; HRMS *m/z* 645.2693 (calcd for $C_{37}H_{41}O_{10}$ 645.2705).

Dichrostachine O (15): yellow oil, $[\alpha]^{20}_D$ −146 (*c* 0.15, MeOH); UV (MeOH) λ_{max} (log ϵ) 208 (4.05), 225 sh (3.95), 256 (3.9), 330 (3.34) nm; IR ν_{max} (film) 3365, 1730, 1660, 1603, 1153, 1025, 764 cm^{-1}; ^1H NMR ($CD_3OD/CDCl_3$, 9;1, 500 MHz) δ 6.5 (1H, d, J = 2 Hz, H-8′), 6.3 (1H, d, J = 2 Hz, H-6′), 6.1 (1H, s, H-3′), 5.34 (1H, d, J = 1.1 Hz, H-3″), 5.23 (2H, m, H-14, H-17), 4.98 (1H, br d, J = 4 Hz, H-5″), 4.82 (1H, br s, H-17), 3.75 (3H, s, OMe), 3.53 (1H, dt, J = 4.6, 8.3 Hz, H-6″), 3.28 (1H, dd, J = 11, 5.3 Hz, H-7), 3.11 (1H, br d, J = 9.4 Hz, H-12), 2.46 (1H, m, H-15), 2.11 (1H, m, H-15), 1.8 (3H, br s, H-16), 0.79 (1H, d, J = 12 Hz, H-9), 0.69 (3H, s, H-18), 0.62 (3H, s, H-19), 0.56 (3H, s, H-20), 0.17 (1H, dd, J = 13, 2 Hz, H-5); ^{13}C NMR, see Table 2; HRMS 603.2962 *m/z* (calcd for $C_{36}H_{43}O_8$ 603.2963).

Dichrostachine P (16): yellow oil, $[\alpha]^{20}_D$ 6 (*c* 0.05, MeOH); UV (MeOH) λ_{max} (log ϵ) 210 (4.16), 225 sh (4.04), 254 (3.96), 330 (3.54) nm; IR ν_{max} (film) 3370, 1685, 1655, 1614, 1168, 758 cm^{-1}; ^1H NMR (CD_3OD, 500 MHz) δ 6.89 (1H, dd, J = 10, 2.2 Hz, H-2″), 6.48 (1H, d, J = 2 Hz, H-8′), 6.3 (1H, br s, H-3′), 6.29 (1H, d, J = 2 Hz, H-6′), 5.98 (1H, d, J = 10 Hz, H-3″), 5.42 (1H, m, H-14), 5.22 (1H, br s, H-17), 4.81 (1H, br s, H-17), 4.59 (1H, br s, H-5″), 3.37 (1H, m, H-6″), 3.28 (1H, dd, J = 11, 5 Hz, H-7), 2.62 (1H, d, J = 7 Hz, H-12), 2.53 (1H, ddq, J = 19.7, 8.8, 2 Hz, H-15), 1.89 (3H, br s, H-16), 0.72 (3H, s, H-18), 0.69 (3H, s, H-19), 0.58 (3H, s, H-20), 0.35 (1H, br d, J = 11.7 Hz, H-5); ^{13}C NMR, see Table 2; HRMS 573.2840 *m/z* (calcd for $C_{35}H_{41}O_7$ 573.2840).

Dichrostachine Q (17): white gum, $[\alpha]^{20}_D$ +156 (*c* 0.212, MeOH); UV (MeOH) λ_{max} (log ϵ) 210 (4.24), 252 (4.29), 300 (3.71), 330 sh (3.65) nm; IR ν_{max} (film) 3375, 1644, 1603 cm^{-1}; ^1H NMR ($CDCl_3$, CD_3OD, 500 MHz) δ 6.25 (1H, d, J = 2.1 Hz, H-8′), 6.21 (1H, d, J = 2.1 Hz, H-6′), 6.00 (1H, s, H-3′), 5.81 (1H, s, H-3″), 5.47 (1H, br s, H-14), 5.41 (1H, br s, H-17), 4.50 (1H, br s, H-17), 4.37 (1H, dd, 10.3, 1 Hz, H-11), 3.91 (3H, s, OMe), 3.90 (1H, m, H-7), 3.22 (1H, br s, H-6″), 2.89 (1H, d, J = 6.9 Hz, H-12), 2.84 (1H, br d, J = 19.5 Hz, H-15), 2.3 (1H, br d, J = 13 Hz, H-3), 2.11 (1H, dd, J = 9, 5 Hz, H-6), 1.91 (1H, d, J = 10.5 Hz, H-9), 1.74 (3H, br s, H-16), 0.91 (3H, s, H-19), 0.82 (3H, s, H-18), 0.78 (3H, s, H-20); ^{13}C NMR, see Table 2; HRMS *m/z* 617.2724 (calcd for $C_{36}H_{41}O_9$ 617.2556).

Dichrostachine R (18): yellow oil, $[\alpha]^{20}_D$ −78 (*c* 0.05, MeOH); UV (MeOH) λ_{max} (log ϵ) 206 (3.98), 275 sh (3.3) nm; IR ν_{max} (film) 3420, 1730, 1458, 1273, 1123, 1071 cm^{-1}; ^1H NMR (CD_3OD, 500 MHz) δ 7.34 (1H, d, J = 8.3 Hz, H-3″), 6.79 (1H, d, J = 8.3 Hz, H-4″), 6.42 (1H, d, J = 1.8 Hz, H-8′), 6.2 (1H, d, J = 1.8 Hz, H-6′), 4.9 (1H, s, H-17), 4.89 (1H, t, J = 7 Hz, H-12), 4.28 (1H, br s, H-17), 3.76 (2H, m, H-7, H-14), 3.45 (1H, d, J = 16.5 Hz, H-15), 2.7 (1H, dd, J = 16.5, 7.5 Hz, H-15), 1.69 (3H, s, H-16), 1.07 (1H, dd, J = 12.5, 2 Hz, H-5), 0.88 (3H, s, H-19), 0.8 (3H, s, H-18), 0.62 (3H, s, H-20); ^{13}C NMR, see Table 2; HRMS *m/z* 571.2695 (calcd for $C_{35}H_{39}O_7$ 571.2701).

Compound 19: yellow oil, UV λ_{max} 234 nm; ^1H NMR ($CDCl_3$, 500 MHz) δ 6.27 (1H, dd, J = 17.5, 11 Hz, H-14), 5.66 (1H, t, J = 4 Hz, H-12), 5.13 (1H, d, J = 17.5 Hz, H-15), 4.95 (1H, d, J = 11 Hz, H-15), 3.49 (1H, d, J = 11 Hz, H-19), 3.19 (1H, d, J = 11 Hz, H-17), 2.16 (1H, ddd, J = 20, 7.5, 4 Hz H-11), 1.99 (1H, ddd, J = 20, 9.5, 3 Hz H-11), 1.26 (1H, dd, J = 10, 2.3 Hz, H-5), 0.97 (3H, d, J = 7 Hz, H-16), 0.89 (3H, s, H-20), 0.86 (3H, s, H-18); ^{13}C NMR ($CDCl_3$, 75 MHz) δ 142 (C, C-13), 138.6 (CH, C-14), 128.6 (CH, C-12), 109.4 (CH_2, C-15), 72.2 (CH_2, C-19), 48.3 (CH, C-5), 44 (CH, C-9), 38.7 (CH_2, C-1), 38 (C, C-4), 36.5 (C, C-10), 35.3 (CH_2, C-3), 35 (CH, C-8),32 (CH, C-17), 30.7 (CH_2, C-7), 25.2 (CH_2, C-11), 21.3 (CH_2, C-6), 17.9 (CH_3, C-18), 17.8 (CH_2, C-2), 14.5 (CH_3, C-16), 14.4 (CH_3, C-20).

Compound 22. To a CH_2Cl_2 solution of Corey's reagent (440 μL; 0.04 mmol) maintained at −78 °C under an argon atmosphere were sequentially added flavoquinone **21** (34 mg; 0.1 mmol) and methyl communate (32 mg; 0.1 mmol) dissolved in 1 mL of CH_2Cl_2. The temperature was maintained for 1 h, and the reaction medium was progressively warmed to room temperature and stirred for three days. The solvent was evaporated and the residue filtered twice on a silica gel plug. Compound **22** (29 mg, 23%) was obtained as a reddish powder: IR ν_{max} (film) 2935, 1718, 1635, 1448, 1392, 1340, 1222, 1188, 1159, 888 cm^{-1}; ^1H NMR ($CDCl_3$, 500 MHz) δ 6.56 (1H, d, J = 2.3 Hz, H-8′), 6.32 (1H, d, J = 2.3 Hz, H-6′), 5.96 (1H, s, H-3′), 5.42 (1H, s, H-3″), 5.12 (1H, m, H-14), 4.85 (1H, br s, H-17), 4.59 (1H, br s, H-17), 3.93 (3H, s, 5′- or 7′-OMe), 3.90 (6H, s, 5′- or 7′-OMe and 4″-OMe), 3.6 (3H, s, 19-OMe), 3.41 (1H, t, J = 5.8 Hz, H-12), 3.26 (1H, dq, J = 21, 1.5 Hz, H-15), 2.86 (1H, br d, J = 21 Hz, H-15), 2.42 (1H, br d, J = 11.6 Hz, H-7), 1.75 (3H, br s, H-16), 1.18 (3H, s, H-18), 0.4 (3H, s, H-20); ^{13}C NMR, see Table 2; HRMS *m/z* 657.3074 (calcd for $C_{39}H_{45}O_9$ 657.3069).

Compound 23. To a solution of flavoquinone **21** (34 mg; 0.1 mmol) in 1 mL of CH_2Cl_2 was added methyl communate (32 mg; 0.1 mmol; 1 equiv) in 1 mL of CH_2Cl_2. The reaction was followed by HPLC, and after 48 h of stirring at room temperature, the solvent was evaporated to give **23** as a red-orange powder, which was not further purified: IR ν_{max} (film) 2936, 1718, 1646, 1603, 1456, 1388, 1330, 1219, 1156, 1104, 824, 731 cm^{-1}; ^1H NMR ($CDCl_3$, 500 MHz) δ 6.35 (1H, d, J = 2.4 Hz, H-8′), 6.33 (1H, d, J = 2.4 Hz, H-6′), 6.11 (1H, s, H-3′), 6.1 (1H, s, H-3″), 5.23 (1H, m, H-14), 4.86 (1H, br s, H-17), 4.49 (1H, br s, H-17), 3.92 and 3.87 (2 × 3H, s, 5′- and 7′-OMe), 3.86 (3H, s, 4″-OMe), 3.76 (1H, dd, J = 8.8, 2.2 Hz, H-6″), 3.59 (3H, s, 19-OMe), 3.03 (1H, br d, J = 19 Hz, H-15), 2.85 (1H, t, J = 6.5 Hz, H-12), 2.01 (1H, m, H-15), 1.81 (3H, br s, H-16), 1.14 (3H, s, H-18), 0.37 (3H, s, H-20); ^{13}C NMR, see Table 2; HRMS *m/z* 681.3042 (calcd for $C_{39}H_{46}NaO_9$ 681.3034).

Molecular Modeling Calculations. Molecular modeling calculations were performed on a Dell P490 station with an Intel Xeon X5355 (2.66 GHz to 1333 MHz) Quad Core processor. All the possible stereoisomers were built using the Sybyl software builder module version 8.03 from TRIPOS Inc. Molecular mechanic and dynamics calculations were performed using the Sybyl software advance computation module version 8.03 from TRIPOS Inc. The eight possible stereoisomers of **22** and **23** (Figure 1) were subjected to conformational search using the quenched molecular dynamics procedure, with atomic potentials assigned by the Tripos force field and Gasteiger−Hückel charges. In this procedure the molecules were heated to a set temperature (1000 K) for a dynamics run and then "cooked" at this temperature for 100.000 fs. Along the trajectory, the molecular conformations were saved at regular intervals of 50 fs. The set of conformations (2000) represented the possible conformations at the set temperature, assuming that the dynamics was performed long enough to sample the entire range of conformations. The resulting structures were subjected to energy minimization until the energy gradient was lower than 0.001 kcal/mol·Å. Each conformation was "quenched"; that is, the conformation was minimized to the nearest local minimum energy. The ensemble of obtained geometries were ranked on the basis of their conformational energy values and grouped into families according to the rms value of superimposition between all heavy atoms. The lowest energy conformation of each stereoisomer was subsequently analyzed in the light of NMR spectra.

Protein Farnesyl Transferase Assay. The assay was carried out as described.[21] In 96-well microplates and in a final volume of 50 μL, the dichrostachines and SCH-66336 were added to a solution of 50 mM Tris/HCl pH = 7.5, 5 mM $MgCl_2$, 5 mM DTT, 0.1 mM $ZnCl_2$, 0.2% octyl-β-D-glucopyranoside, 10 μM GCVLS-dansyl substrate (Calbiochem, Darmstadt, Germany), and 10 μM farnesyl pyrophosphate (Sigma, St Louis, MO). The reaction was initiated by addition of 10 nM rat PFTase (Jena Biosciences, Jena, Germany). Stock solutions of the natural products were prepared in 100% DMSO at a 10 mM final concentration and diluted in assay buffer to final concentrations ranging from 0.3 nM to 100 μM. Each compound was tested in triplicate and final DMSO % fixed to 1%. Reactions were incubated 30 min at 37 °C, and the fluorescence was read on a NOVOstar (BMG Labtechnologies, Offenburg, Germany) plate reader at 340 nm excitation and 505 nm emission. IC_{50}'s were determined by using the sigmoidal dose−response calculation of the GraphPad Prism software.

Antiproliferative Assay. The metastatic melanoma WM 266-4 cell line was purchased from the ATCC. A total of 5000 cells were seeded per well in 96-well microplates and incubated in RPMI (Lonza) culture medium containing 10% fetal bovine serum (Sigma), 50 μg/mL streptomycin, and 50 U/mL penicillin, during 72 h. Each compound was tested in triplicate and final DMSO % fixed to 1%. The antiproliferative activity was measured using the ATP Lite assay (Perkin-Elmer). The luminescent signal was read on an Envision multimode reader (Perkin-Elmer), and IC_{50}'s were determined by using the sigmoidal dose−response calculation of the GraphPad Prism software.

Acknowledgment. The authors are grateful to Y. Aussagues and V. Poughon for their highly skilled contribution and to Dr. P. Hellier for critical reading of the manuscript.

Supporting Information Available: This material is available free of charge via the Internet at http://pubs.acs.org.

References and Notes

(1) (a) Cox, A. D.; Der, C. J. *Biochim. Biophys. Acta Rev. Cancer* **1997**, *1333*, F51–71. (b) Sebti, S. M.; Hamilton, A. D. *Pharmacol. Ther.* **1997**, *74*, 103–114.

(2) Hara, M.; Akasaka, K.; Akinaga, S.; Okabe, M.; Nakano, H.; Gomez, R.; Wood, D.; Uh, M.; Tamanoi, F. *Proc. Natl. Acad. Sci. U.S.A.* **1993**, *90*, 2281–2285.

(3) Ferri, N.; Yokoyama, K.; Sadilek, M.; Paoletti, R.; Apitz-Castro, R.; Gelb, M. H.; Corsini, A. *Br. J. Pharmacol.* **2003**, *138*, 811–818.

(4) Lee, S.; Park, S.; Oh, J. W.; Yang, C. *Planta Med.* **1998**, *64*, 303–308.

(5) Palgrave K. C. *Trees of Southern Africa*, 4th ed.; C. Struik Publishers: Cape Town, 1984; p 254.

(6) (a) Arbonnier, M. *Arbres, arbustes et lianes des zones sèches d'Afrique de l'Ouest*, 2nd ed.; CIRAD-MNHN Éditions: Paris, 2002; p 386. (b) Bouquet, A. *Féticheurs et médecines traditionnelles du Congo (Brazzaville)*; ORSTOM: Paris, 1969; p 164. (c) Kerharo, J.; Adam, J. G. *La Pharmacopée sénégalaise traditionnelle, Plantes médicinales et toxiques*; Vigot Frères: Paris, 1974; pp 573−575. (d) Adjanohoun, E. J.; Ahyi, A. M. R. *Médecine traditionnelle et pharmacopée, contribution aux études ethnobotaniques et floristiques en République Populaire du Congo*; Agence de Coopération Culturelle et Technique: Paris, 1986; pp 220−221. (e) Adjanohoun, E. J.; Ahyi, A. M. R. *Médecine traditionnelle et pharmacopée, contribution aux études ethnobotaniques et floristiques en République Populaire du Congo*; Agence de Coopération Culturelle et Technique: Paris, 1988; pp 248−249.

(7) (a) Abou Zeid, A. H. S.; Hifnawy, M. S.; Mohamed, R. S. *Planta Med.* **2008**, *74*, 1020–1021. (b) Fotie, J.; Nkengfack, A. E.; Peter, M. G.; Heydenreich, M.; Fomum, Z. T. *Bull. Chem. Soc. Ethiopia* **2004**, *18*, 111–115. (c) Jain, R.; Saxena, U. *J. Ind. Chem. Soc.* **2003**, *80*, 656–658.

(8) Clark-Lewis, J. W.; Dainis, I. *Aust. J. Chem.* **1968**, *21*, 425–437.

(9) Chung, S.-K.; Kim, Y.-C.; Takaya, Y.; Terashima, K.; Niwa, M. *J. Agric. Food Chem.* **2004**, *52*, 4664–4668.

(10) Noma, M.; Suzuki, F.; Gamou, K.; Kawashima, N. *Phytochemistry* **1982**, *21*, 395–397.

(11) Hauteville, M.; Chopin, J.; Geiger, H.; Schüler, L. *Tetrahedron Lett.* **1980**, *21*, 1227–1230.

(12) Lin, A. S.; Chang, F. R.; Wu, C. C.; Liaw, C. C.; Wu, Y. C. *Planta Med.* **2005**, *71*, 867–70.

(13) For intramolecular reactivity, see: Kharitonov, Y. V.; Shults, E. E.; Shakirov, M. M.; Tolstikov, G. A. *Russ. J. Org. Chem* **2005**, *41*, 1145–1157.

(14) Vilegas, W.; Filecio, J.; Roque, N. F.; Gottlieb, H. E. *Phytochemistry* **1991**, *30*, 1869–1872.

(15) Pinto, A. C.; Pizzolatti, M. G.; Epifanio, R.; Frankmölle, W.; Fenical, W. *Tetrahedron* **1997**, *53*, 2005–2012.

(16) Laroche, M.-F.; Marchand, A.; Duflos, A.; Massiot, G. *Tetrahedron Lett.* **2007**, *48*, 9056–9058.

(17) Hörhammer, L.; Wagner, H.; Rösler, H.; Keckeisen, M.; Farkas, L. *Tetrahedron* **1965**, *21*, 969–975.

(18) Mangoni, L.; Belardini, M. *Gazz. Chim. Ital.* **1964**, *94*, 1108–1121.

(19) Ryu, D. H.; Zhou, G.; Corey, E. J. *J. Am. Chem. Soc.* **2004**, *126*, 4800–4802.

(20) Liu, M.; Bryant, M. S.; Chen, J.; Lee, S. N.; Yaremko, B.; Lipari, P.; Malkowski, M.; Ferrari, E.; Nielsen, L.; Prioli, N.; Dell, J.; Sinha, D.; Syed, J.; Korfmacher, W. A.; Nomeir, A. A.; Lin, C. C.; Wang, L.; Taveras, A. G.; Doll, R. J.; Njoroge, F. G.; Mallams, A. K.; Remiszewski, S.; Catino, J. J.; Girijavallabhan, V. M.; Kirschmeier, P.; Bishop, W. R. *Cancer Res.* **1998**, *58*, 4947–4956.

(21) Ledroit, V.; Debitus, C.; Ausseil, F.; Raux, R.; Menou, J. L.; Hill, B. T. *Pharm. Biol.* **2004**, *42*, 454–456.

NP900095Z